










Phosphorylation status of B β subunit acts as a switch to regulate the function of phosphatase PP2A in ethylene-mediated root growth inhibition

Zhengyao Shao^{1,2} , Bo Zhao^{1,2} , Prashanth Kotla¹ , Jackson G. Burns¹ , Jaclyn Tran^{1,2} , Meiyu Ke³ , Xu Chen³ , Karen S. Browning^{1,2}  and Hong Qiao^{1,2} 

¹Institute for Cellular and Molecular Biology, The University of Texas at Austin, Austin, TX 78712, USA; ²Department of Molecular Biosciences, The University of Texas at Austin, Austin, TX 78712, USA; ³Haixia Institute of Science and Technology, Horticultural Plant Biology and Metabolomics Center, Fujian Agriculture and Forestry University, Fuzhou, Fujian 350002, China

Summary

Author for correspondence:
Hong Qiao
Email: hqiao@austin.utexas.edu

Received: 12 May 2022
Accepted: 25 August 2022

New Phytologist (2022) **236**: 1762–1778
doi: 10.1111/nph.18467

Key words: *Arabidopsis thaliana*, ethylene signalling, PP2A, protein complex, protein phosphorylation, root development.

- The various combinations and regulations of different subunits of phosphatase PP2A holoenzymes underlie their functional complexity and importance. However, molecular mechanisms governing the assembly of PP2A complex in response to external or internal signals remain largely unknown, especially in *Arabidopsis thaliana*.
- We found that the phosphorylation status of B β of PP2A acts as a switch to regulate the activity of PP2A. In the absence of ethylene, phosphorylated B β leads to an inactivation of PP2A; the substrate EIR1 remains to be phosphorylated, preventing the EIR1-mediated auxin transport in epidermis, leading to normal root growth.
- Upon ethylene treatment, the dephosphorylated B β mediates the formation of the A2–C4–B β protein complex to activate PP2A, resulting in the dephosphorylation of EIR1 to promote auxin transport in epidermis of elongation zone, leading to root growth inhibition.
- Altogether, our research revealed a novel molecular mechanism by which the dephosphorylation of B β subunit switches on PP2A activity to dephosphorylate EIR1 to establish EIR1-mediated auxin transport in the epidermis in elongation zone for root growth inhibition in response to ethylene.

Introduction

Ethylene is a gaseous phytohormone that regulates various developmental processes and protects plants from both biotic and abiotic stress (Fukao *et al.*, 2006; Xu *et al.*, 2006; Achard *et al.*, 2007; Boutrot *et al.*, 2010; Licausi *et al.*, 2010; Mersmann *et al.*, 2010; Ma *et al.*, 2013; Broekgaarden *et al.*, 2015; Hartman *et al.*, 2019; Marhavý *et al.*, 2019; Pandey *et al.*, 2021). The ethylene signal is perceived on the endoplasmic reticulum (ER) membrane (Chang *et al.*, 1993; Hua & Meyerowitz, 1998; Hua *et al.*, 1998; Chang & Bleecker, 2004). ETHYLENE INSENSITIVE 2 (EIN2), a key mediator of ethylene signalling, transduces the ethylene signal from the ER to the nucleus via dephosphorylation, cleavage, and nuclear translocation of its C-terminal domain (EIN2-C) (Kieber *et al.*, 1993; Alonso *et al.*, 1999; Ju *et al.*, 2012; Qiao *et al.*, 2012). In the nucleus, EIN2-C and the transcription factor ETHYLENE INSENSITIVE 3 (EIN3) interact with EIN2 NUCLEAR INTERACTING PROTEIN 1 (ENAP1) to regulate histone acetylation and ethylene-induced transcription (Zhang *et al.*, 2016a, 2017; Wang *et al.*, 2017). The positive feedback regulation that results from EIN3 dimerisation is required for both histone acetylation and gene expression that regulates transcription of ethylene-responsive genes (Wang *et al.*,

2020b). EIN3 modulates a multitude of downstream transcriptional cascades, including a major feedback regulatory circuitry of the ethylene signalling pathway, and integrates numerous connections between hormone-mediated, growth-response pathways (Chao *et al.*, 1997; Guo & Ecker, 2003; Chang *et al.*, 2013). The positive regulatory role of EIN3 in ethylene signalling is well characterised, and more recently EIN3 has been shown to repress gene expression by interacting with a transcription repressor specifically regulated by ethylene (Wang *et al.*, 2020a).

Responses to ethylene induce various morphological changes that allow plant adaptation to the ever-changing external environment (Jackson, 2008; Steffens *et al.*, 2012; Dubois *et al.*, 2015; Qing *et al.*, 2016; Shi *et al.*, 2016; Haydon *et al.*, 2017; Wu *et al.*, 2020; Gong *et al.*, 2021). Seedlings germinated in the dark in the presence of saturated concentrations of ethylene display a characteristic phenotype known as the triple response, which includes the exaggeration of the curvature of apical hooks and the shortening and thickening of hypocotyls and roots (Ecker, 1995; Bleecker & Kende, 2000). How ethylene inhibits root growth has been a longstanding question. It is known that ethylene-mediated inhibition of root cell proliferation at the root apical meristem is mainly achieved by restricting epidermal cell expansion (Street *et al.*, 2015; Vaseva *et al.*, 2018). and that ethylene

stimulates auxin biosynthesis and basipetal auxin transport toward the elongation zone, where it activates a local auxin response leading to the inhibition of cell elongation (Růžička *et al.*, 2007; Brumos *et al.*, 2018). The current model is that ethylene stimulates auxin biosynthesis in the root tip and auxin transport in the lateral root cap (LRC) and epidermis by AUX1 and PIN-FORMED 2 (PIN2) (Růžička *et al.*, 2007; Swarup *et al.*, 2007). A recent study showed that ethylene stimulates auxin biosynthesis and transport in the epidermis, which is the key step to mediate root growth inhibition, and this epidermis-specific signalling has an impact on the growth of neighbouring cells (Vaseva *et al.*, 2018). However, how ethylene stimulates the auxin transport is unknown. Růžička *et al.* (2007) showed that ethylene promotes the expression of AUX1 and PIN2 (Růžička *et al.*, 2007), but elevation is relatively limited, and therefore unlikely to play a substantial role in regulating auxin transport in the ethylene response. One possibility is that these proteins are activated through ethylene-mediated post-translational regulation.

Protein phosphorylation is one of the most important post-translational regulations that has been showed to play important functions in ethylene-mediated root growth inhibition. In the absence of ethylene, the kinase CONSTITUTIVE TRIPLE RESPONSE 1 (CTR1) phosphorylates EIN2-C, leading to an inactivation of EIN2, resulting in a normal root growth (Clark *et al.*, 1998; Gao *et al.*, 2003; Ju *et al.*, 2012). In the presence of ethylene, EIN2-C is dephosphorylated by an unknown mechanism, resulting in cleavage and nuclear translocation of EIN2-C, leading to root growth inhibition. The phosphorylation of aminocyclopropane-1-carboxylic acid (ACC) synthases by mitogen-activated protein kinase (MAPK) and calcium-dependent protein kinase (CDPK) stabilises the ACC synthases and therefore promotes the synthesis of ACC, the precursor of ethylene that induces the root growth inhibition (Joo *et al.*, 2008; Han *et al.*, 2010; Li *et al.*, 2012). Furthermore, the phosphorylation of CAP BINDING PROTEIN 20 (CBP20) at Ser245 stimulated by ethylene treatment represses MYB DOMAIN PROTEIN 33 (MYB33) expression through miR319b to inhibit root growth (Zhang *et al.*, 2016b). Most of kinases and phosphatases that are involved in ethylene-mediated regulation are still unidentified, and the molecular mechanisms by which the enzymatic activities of these proteins for particular substrate proteins are fine-tuned are largely unknown.

In this study, we demonstrated that the phosphorylation status of B β , the regulatory subunit of the PROTEIN PHOSPHATASE 2A (PP2A), acts as a switch to regulate the activity of the phosphatase in dephosphorylation of the auxin transporter ETHYLENE INSENSITIVE ROOT 1 (EIR1) (Luschnig *et al.*, 1998; Alonso *et al.*, 2003), promoting auxin transport in epidermis in elongation zone to inhibit root growth in response to ethylene. We found that the PP2A catalytic subunit C4 can interact with the regulatory subunit B β and the scaffolding subunit A2 both *in vitro* and *in vivo* to form a protein complex. In the absence of ethylene, B β is phosphorylated, whereas in the presence of ethylene, B β is dephosphorylated, leading to the formation of A2–C4–B β complex. Furthermore, both our genetics and biochemistry experiments demonstrated that EIR1 is the target of

PP2A and that the interaction between EIR1 and the PP2A complex is mediated by A2. In the absence of ethylene, the phosphorylation of B β results in inactivation of PP2A, and EIR1 remains phosphorylated, preventing the EIR1-mediated auxin transport to the epidermis; as a result, no root growth inhibition occurs. By contrast, in the presence of ethylene, the dephosphorylation of B β leads to an activation of PP2A phosphatase to dephosphorylate EIR1, promoting the EIR1 mediated auxin transport in epidermis; as a result, the root growth is inhibited. Taken together, our research reveals the novel molecular mechanism through which ethylene signalling regulates EIR1 phosphorylation through B β dephosphorylation to active EIR1-mediated auxin transport in epidermis in elongation zone, leading to root growth inhibition.

Materials and Methods

Plant materials, growth condition and hormone responses

Arabidopsis (*Arabidopsis thaliana*) accession Columbia (Col-0) was used as the wild-type for all the experiments and all of the mutant genotypes in this ecotype background were used. The T-DNA insertion mutants of *pp2a-a2-1* (or *a2-1*, At3G25800, SALK_042724) (Zhou *et al.*, 2004), *pp2a-b β -1* (or *b β -1*, At1G17720, SALK_062514), *pp2a-c4-1* (or *c4-1*, At3G58500, SALK_035009) (Spinner *et al.*, 2013), *eir1* (AT5G57090, SALK_144447.43.90.x) (Chang *et al.*, 2019), and the point mutation mutant *eir1-1* (CS8085) (Roman *et al.*, 1995) were ordered from Arabidopsis Biological Resource Center. The T-DNA insertions of *a2-1*, *b β -1*, *c4-1*, and *eir1* (SALK_144447.43.90.x) were confirmed by genotyping PCR to identify the homozygotes; the *eir1-1* homozygotes were genotyped by Derived Cleaved Amplified Polymorphic Sequences (dCAPS) method (Neff *et al.*, 1998). Primers are listed in Table S1. Seeds were surface sterilised with 50% bleach and 0.01% Triton X-100 for 10 min, washed with sterile distilled water for four times, sown on Murashige & Skoog medium plates containing 1% sucrose and 1% phytoblend and stratified for 3 d at 4°C in the dark. For seed propagation, after germination under light, green seedlings were transferred into soil (Promix-HP) and grown in a growth chamber setting with the long-day photoperiod (16 h : 8 h, light : dark) at 22°C until maturity.

The etiolated seedling triple response assay was performed with sterilised seeds on various concentrations of 1-aminocyclopropane-1-carboxylic acid (ACC; Sigma) plates (0, 2, 5 and 10 μ M ACC). After 3 or 4 wk upon seed harvesting, *c.* 50 seeds of each genotype collected at the similar time were plated on the same Murashige & Skoog (MS) medium plate per concentration. ACC plates with seeds were placed at 4°C in the dark for 3 d for stratification and then were exposed to light for 4 h and put in the dark for another 3 d at 22°C. For phenotypic analysis, representative seedlings from each genotype were selected and placed horizontally on the MS plate and then photographed against a black background. Their root lengths were measured using Fiji IMAGEJ software (Schindelin *et al.*, 2012).

For all protein assays, ethylene treatment of *Arabidopsis* etiolated seedlings was performed with sterile seeds growing on MS plates. After stratification and light exposure, MS plates with seeds were placed in air-tight containers in the dark with a flow of hydrocarbon-free air at 22°C for 3 d. Those etiolated seedlings were subsequently treated with ethylene gas at 10 ppm or hydrocarbon-free air for 4 h before sampling.

Transient expression in *Nicotiana benthamiana* leaves and in protoplasts

Here, 20 ml overnight cultures of *Agrobacterium tumefaciens* (strain GV3101) in Luria–Bertani (LB) medium carrying the binary vectors were pelleted by centrifuge at 2000 *g* at room temperature (RT) for 15 min and then resuspended in infiltration buffer (10 mM MgCl₂, 10 mM MES, pH 5.7, and 100 μM acetosyringone, AS). According to different experiment procedures, pairs of resuspended *Agrobacterium* cultures were combined and then mixed with an equal volume of p19 resuspension to reach a final OD₆₀₀ of 0.8 for each resuspension before the infiltration at the abaxial side of *N. benthamiana* leaves using a needleless syringe. After growth for 2 or 3 d under dim light condition, infected *Nicotiana benthamiana* leaves were collected and snap frozen in LN₂ for further protein analysis.

Next, 4-wk-old *Arabidopsis* plants grown in soil in growth chamber were used for protoplast isolation and the transient expression assay performed according to previous publication (Yoo *et al.*, 2007). For protoplast-based transient expressions, protoplasts were transfected with a combination of constructs (*c.* 100 μg plasmid DNA in total for 1 ml protoplasts for each sample) and incubated at RT in the dark for 8 h. ACC was added into the protoplast to reach a final concentration of 10 μM after 4 h of incubation. After 4 h ACC treatment, protoplasts were harvested by centrifugation at low speed and snap frozen in LN₂ for further experiments.

Plasma membrane protein extraction

For EIR1 detection, root tissues from 3-d-old etiolated seedlings undergoing air or C₂H₄ treatment were harvested and homogenised in LN₂ to a powder. Total membrane extraction was performed as previously described (Abas & Luschnig, 2010; Leitner & Luschnig, 2014; Avila *et al.*, 2015). In brief, homogenised root materials or pelleted protoplasts were first resuspended in pre-chilled 1× extraction buffer (50 mM Tris–HCl, pH 8.8, 150 mM NaCl, 1 mM EDTA, 10% (v/v) glycerol, 1 mM phenylmethanesulfonylfluoride (PMSF) and 1× protease inhibitor cocktail) with a combination of phosphatase inhibitors (20 mM NaF, 1 mM Na₂MoO₄, 10 mM Na₃VO₄, 50 mM β-glycerophosphate and 1× PhosStop cocktail (Roche)) to preserve EIR1 phosphorylation status. After the addition of equilibrated polyvinylpyrrolidone (PVPP) suspension, the total homogenate was centrifuged and cleared at 4°C (2 min, 500 *g*). Following a one time repeat of the extraction with the same volume of extraction buffer, the re-extracted supernatant was combined with the first extract and centrifuged at 4°C for 2 h at 22 000 *g* to

obtain a total membrane pellet. For EIR1 western blot detection, sample pellets were solubilised with sodium dodecyl sulfate–polyacrylamide gel electrophoresis (SDS–PAGE) sample buffer containing 8 M urea and 5% SDS and denatured at 50°C for 5 min to prevent protein aggregation. For EIR1-related immunoprecipitation (IP), 0.2 ml of membrane solubilisation buffer (100 mM Tris–HCl, pH = 7.3, 150 mM NaCl, 1 mM EDTA, 10% glycerol, 20 mM NaF, 1% Triton X-100, 1 mM Na₂MoO₄, 10 mM Na₃VO₄, 50 mM β-glycerophosphate and 1× PhosStop cocktail, 1 mM PMSF, 1× protease inhibitor cocktail) was added to the membrane pellet followed by full resuspension. Insoluble particles were removed by centrifugation for 2 min at 22 000 *g* at 4°C. The precleared supernatant containing solubilised proteins was used for the following IP experiments.

Co-immunoprecipitation and immunoblot assays

For co-immunoprecipitation (co-IP), *c.* 2–3 g of plant material were ground in a prechilled mortar with liquid nitrogen. Soluble total proteins were extracted in two volumes of co-IP buffer (50 mM Tris–Cl, pH 8, 150 mM NaCl, 1 mM EDTA, 0.1% Triton X-100, 1 mM PMSF and 1× protease inhibitor cocktail) at 4°C for 15 min with gentle rocking. The lysates were cleared by centrifugation at 4°C (10 min, 5000 *g*). The antibody used for immunoprecipitation was prebound with the equilibrated protein-G coated magnetic beads (Dynabeads; Thermo Fisher, Waltham, MA, USA) for 3 h with gentle rotation at 4°C. A 10% input aliquot for each co-IP experiment was taken from the cleared supernatant before the rest of the supernatant was added to Dynabeads and incubated at 4°C with gentle rocking overnight. Dynabeads were precipitated magnetically using a DynaMagnetic rack (Thermo Fisher) and then washed five times with 0.5 ml of co-IP buffer. Proteins were then released from the Dynabeads using 2× Laemmli sample buffer by heating at 85°C for 8 min.

For protein immunoblots, proteins were separated by SDS–PAGE and transferred to a nitrocellulose membrane (0.2 μm; Bio-Rad) using the wet-tank transfer method and blocked with 5% nonfat milk in Tris-buffered saline Tween (TBST) for 1 h at RT before the overnight inoculation in primary antibody at 4°C with gentle rotation. For analysis of the EIR1 phosphorylation state, the stacking gel contains 3 M urea and the 7% running gel was used and run for 3 h at 120 V at 4°C. After transfer, the nitrocellulose membranes were blocked in 5% BSA in TBST for 2 h at RT before immunoblotting. The following antibodies and dilutions were used for immunoblotting: anti-HA (#901503; Biolegend, San Diego, CA, USA), 1 : 10 000; anti-Myc (#2276; CST), 1 : 2000; anti-FLAG (rabbit) (#14793; CST), 1 : 2000; and anti-FLAG (mouse) (F3165; Sigma), 1 : 5000. Goat anti-mouse Kappa Light Chain antibody (#105001G; Bio-Rad) and goat anti-rabbit (IgG (H + L)–horseradish peroxidase (HRP) conjugate #1706515; Bio-Rad) were used as secondary antibodies at 1 : 10 000 dilution. Native EIR1 primary antibody was generated by affinity purification of rabbit serum containing EIR1 antibody, kindly provided by Christian Luschnig. HRP activity was detected using enhanced chemiluminescence (ECL; GE

Healthcare, Heights, IL, USA) according to the manufacturer's instructions with either a ChemiDoc Imaging System (Bio-Rad) or conventional X-ray films.

In vitro EIR1-hydrophilic loop (HL) phosphorylation assays and calf intestinal alkaline phosphatase (CIP) treatment

Recombinant GST–EIR1–HL proteins were expressed in the *E. coli* strain BL21 with protein induction when OD₆₀₀ reached 0.5 with 1 mM isopropyl β-D-1-thiogalactopyranoside (IPTG) for 4 h at 37°C and then purified over a glutathione Sepharose 4B column (GE Healthcare). The eluted samples were then resolved by SDS-PAGE and stained with Coomassie brilliant blue R-250 to evaluate purity. The *in vitro* EIR1-HL phosphorylation was performed as previously described (Michniewicz *et al.*, 2007). In brief, crude plant lysates were extracted from homogenised root tissues using 100 µl extraction buffer (20 mM Tris–HCl, pH 7.5, 150 mM NaCl, 0.5% Tween-20, 1 mM DTT, 1× PMSF, and 1× protease inhibitor cocktail) per sample. Here, *c.* 1 µg of purified GST–EIR1–HL was mixed with kinase buffer (20 mM Tris, pH 7.5, 10 mM MnCl₂, 1 mM ATP and 1 mM DTT) containing 1 µCi of (γ-³²P) ATP to a final volume of 10 µl. This was added into 10 µl crude plant extracts. Reactions were incubated at 30°C for 30 min. Reactions were terminated by the addition of 2× SDS loading buffer. After denaturation at 95°C for 2 min, proteins were resolved on 4–20% stain-free pre-cast gels (Bio-Rad). Either directly after electrophoresis or after Coomassie brilliant blue R250 staining, destaining and drying, the gels were exposed to phosphor screens and the autoradiograph signals were detected using the Typhoon FLA 9500 system.

For CIP treatment of samples, the membrane pellet from root tissue was first washed five times in extraction buffer without EDTA and phosphatase inhibitors five times. Then, the pellet was resuspended fully in 50 µl CIP buffer (100 mM NaCl, 50 mM Tris–HCl, pH 7.9, 10 mM MgCl₂, 1 mM DTT) and treated with 2 units of CIP (NEB) at 37°C for 15 min. The reaction was stopped by adding 10 µl 6× loading buffer followed by denaturation at 50°C for 5 min. Proteins were resolved on a 7% SDS-PAGE gel.

Quantification and statistical analysis

Details of statistical analyses can be found in the figure legends. R package DPLYR was used to perform statistical analyses for phenotypic assays.

CRISPR-Cas9 mutagenesis

The *a2-1c4-2* and *a2-1c4-3* double mutants were generated using the CRISPR-Cas9 system in *a2-1* single mutant background by following a previous publication (Wang *et al.*, 2015; Minkenberg *et al.*, 2019). In brief, pairs of two guide RNA (gRNA) sequences targeting *C4* coding region were designed using CRISPR-PLANT v.2 (<http://omap.org/crispr2/index.html>) online tool. gRNA sequences with high specificity in the *Arabidopsis* genome and

predicted efficiency were chosen for PCR amplification using the pDT1T2 vector as the template and later incorporated into the binary vector pHEE401E. The *Agrobacterium*-mediated floral dipping method was used to transform the pHEE401E vector containing *C4* gRNA into *a2-1* plants. Genomic DNAs extracted from hygromycin-positive T1 plants were used for genotyping and followed by Sanger sequencing to detect the CRISPR-Cas9 directed mutation and obtain double homozygotes of *a2-1c4-2* and *a2-1c4-3*.

GFP fluorescence quantification

The quantification of *DR5::GFP* fluorescence in ethylene and ACC treatment was performed using IMAGEJ FIJI software (<https://imagej.net/software/fiji/>). Boxes were drawn surrounding the epidermis in the root elongation zone as the area of interest, illustrated in Fig. 6(e) (please refer to later paragraphs), symmetrically against the root axis. Integrated fluorescence intensity and area value were measured for each individual plants and calculated to give the mean value for plotting. The significance of differences between different genetic backgrounds and treatment groups were calculated using Student's *t*-test.

Gravitropic response assay

Here, 5-d-old seedlings grown on MS medium supplied with 1% sucrose under long-day light cycle were used. Plants were transferred to a new vertical plate and aligned before the gravistimulation. Pictures were taken 24 h after the gravitropism assays and the root bending angles were quantified using IMAGEJ FIJI software with the angle tool function.

Single nucleus RNA sequencing (sNucRNA-seq) data processing

The sNucRNA-seq of *Arabidopsis* root tissue was obtained from a previous publication under accession number GSE155304. Integrated sNucRNA-seq rds file (GSE155304_rnaseq_integration.rds.gz) was used for further analysis of the PP2A and EIR1 expression profiles. Dot plot and UMAP were generated using the SEURAT R package (v.2.3.4) with adaptation. Cluster-specific marker genes of trichoblast and atrichoblast cell types were selected based on previous publications (Butler *et al.*, 2018; Farmer *et al.*, 2021).

Results

Ethylene-induced dephosphorylation of Bβ is involved in the regulation of root growth

Protein phosphorylation is one of the most important post-translational regulations that has been showed to play important functions in ethylene-mediated root growth inhibition. In the survey of ethylene-regulated phosphoproteomics, we found that, in the absence of ethylene, the Bβ subunit was phosphorylated at serine 460; whereas, in the presence of ethylene, the Bβ

subunit was completely dephosphorylated (Figs 1a, S1a). The regulatory B subunits of PP2A have been reported to serve as targeting signals for substrate recruitment and phosphatase activity (Rodgers *et al.*, 2011; Tang *et al.*, 2011). We first examined the expression of *B β* in its native promoter-driven GUS (*proB β ::GUS*) transgenic plants. We found that *B β* was expressed across all the plant tissues and its expression was not altered by ethylene (Fig. S1b). No obvious ethylene-responsive phenotype was detected from the T-DNA knock-out *B β* plants (Fig. S1c–e). To further evaluate whether the B β phosphorylation status change plays any role in the ethylene response, we generated the plants that contained a wild-type B β (*B β ox*), the plants that contained a phospho-mimic form of B β (*B β ^{S460E}ox*) and the plants with a phospho-dead form of B β (*B β ^{S460A}ox*). Independent transgenic lines with a comparable protein expression of B β , B β ^{S460E} or B β ^{S460A} were obtained (Fig. S1d) and used for phenotypic analysis. Compared with Col-0, the overexpression of wild-type *B β* did not display an obvious alteration in ethylene-responsive phenotype (Fig. 1b,c). However, *B β ^{S460E}ox* plants displayed an ethylene insensitive phenotype. By contrast, *B β ^{S460A}ox* plants displayed a hyperethylene sensitive phenotype, specifically in roots, even in the absence of ACC (Fig. 1b,c). These results suggest that the phosphorylation of B β at Ser460 negatively regulates ethylene-mediated root growth inhibition, whereas the dephosphorylated B β at Ser460 plays a positive role in the ethylene-mediated root growth inhibition.

B β is in the same protein complex as PP2A subunits A2, C4, and B β phosphorylation status regulates the complex formation

The heterotrimeric protein phosphatase 2A (PP2A) is a protein serine/threonine phosphatase composed of a scaffolding subunit (A), a catalytic subunit (C) and a regulatory subunit (B). The various compositions of different PP2A holoenzymes underlie their functional complexity in cell division, morphogenesis, hormone signalling, and stress response (DeLong, 2006; Skottke *et al.*, 2011; Spinner *et al.*, 2013; Uhrig *et al.*, 2013; Bian *et al.*, 2020). To investigate whether there is a distinct combination of A and C subunits acting collectively with the B β subunit in the ethylene response, we first performed a yeast-two-hybrid screening using B β as bait protein. We found that the B β subunit interacted with the C4 subunit and that C4 interacted with the A2 subunit (Fig. S2a,b). The interaction was further confirmed by the semi-*in vivo* assay using A2, B β and C4 transiently expressed in tobacco leaves (Fig. 2a,b). To examine whether A2 and C4 are associated with B β *in planta* spatially, we examined the gene expression profiles of A2, C4 using eFP provided by TAIR website (Fig. S2c,e). Both of them were expressed across all the tissues, showing that they shared a similar expression pattern with B β (Fig. S2c–e).

To examine whether and how these subunits interact *in vivo* and to determine whether ethylene influences their interactions, we generated transgenic plants containing both C4-YFP-HA and A2-FLAG-GFP, or both C4-YFP-HA and B β -Myc. Then

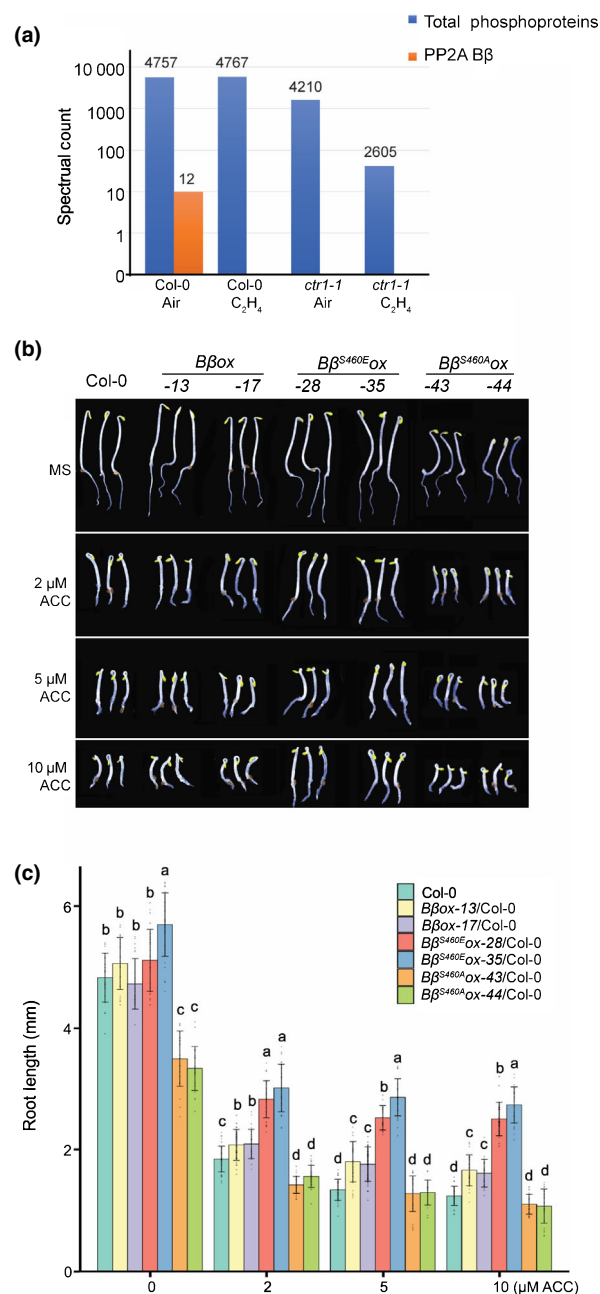


Fig. 1 *Arabidopsis* PP2A-B β is dephosphorylated at Ser460 upon ethylene treatment, which is involved in ethylene-mediated root growth. (a) Spectral counts of phosphorylated PP2A-B β peptides in Columbia (Col-0) or *ctr1-1* mutants treated with 4 h of air or ethylene gas. Spectral counts were calculated by averaging three biological replicates. Total spectral counts of all phosphoproteins in each sample serve as an internal control. (b) The seedling phenotypes of overexpression of different formats of B β subunit. Wild-type *B β* , the phospho-mimic *B β ^{S460E}*, and phospho-dead *B β ^{S460A}* were transformed onto the Col-0 background. Two independent transgenic lines from each transformation with similar B β protein expression levels were selected for phenotypic analysis. The seedlings were grown on Murashige & Skoog (MS) medium containing 2, 5 or 10 μ M aminocyclopropane-1-carboxylic acid (ACC) or without ACC in the continuous dark before being photographed. (c) Measurements of the root lengths from the indicated etiolated seedlings described in (b). Values are means \pm SD of at least 30 seedlings. Different letters indicate significant differences between different genotypes calculated using a two-tailed *t*-test with $P \leq 0.05$. Individual data points are plotted.

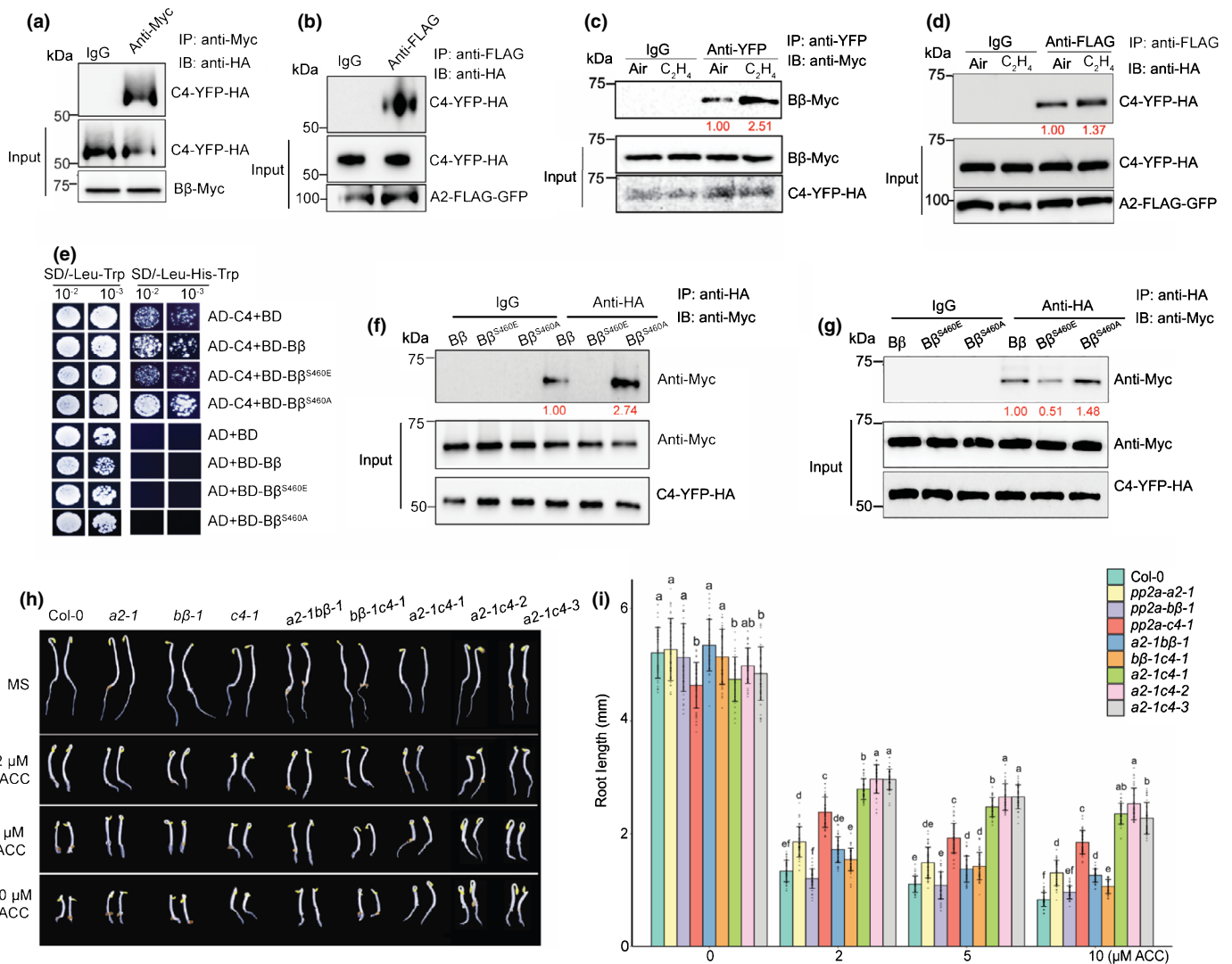


Fig. 2 A2, B β and C4 subunits are in the same protein complex that is involved in ethylene-mediated root growth inhibition in *Arabidopsis*. (a, b) Pull-down assays of B β (B β -Myc) with C4 (C4-YFP-HA) (a) and A2 (A2-FLAG-GFP) with C4 (b) transiently expressed in *Nicotiana benthamiana* leaves. (c, d) *In vivo* co-immunoprecipitation assays of B β with C4 and A2 with C4. The total protein extracts from seedlings of crossed *B β ox-C4ox* (c) or *A2ox-C4ox* (d) F1 transgenic plants treated with 4 h of air or ethylene were immunoprecipitated with anti-HA or anti-FLAG, respectively. The co-immunoprecipitated proteins were detected by western blotting using either anti-Myc or anti-HA. The input serves as the loading control. The red numbers indicate the quantitation value from anti-Myc or anti-HA divided by the input control. IB, immunoblotting; IP, immunoprecipitation. (e) Yeast two-hybrid assay to examine the interaction between C4 with the full length coding sequence (CDS) of B β , the phospho-mimic B β ^{S460E}, and the phospho-dead B β ^{S460A}. AD, GAL4 activation domain; BD, GAL4 DNA binding domain. Left panels: Yeasts grown on two-dropout medium as a control. Right panels: yeast grown on selective three-dropout medium. (f) Pull-down assays to examine the interaction between C4 with B β , B β ^{S460E}, or B β ^{S460A}. Reactions were performed using total plant extracts from *N. benthamiana* transiently co-expressed C4-YFP-HA with B β -Myc, or B β ^{S460E}-Myc, or B β ^{S460A}-Myc respectively. Red numbers indicate B β -Myc and B β ^{S460E}-Myc band intensities normalised to their corresponding input band signals, respectively. (g) *In vivo* co-immunoprecipitation assays to detect the interaction between C4 and different formats of B β . Reactions were performed using total protein extracts from Columbia (Col-0) protoplasts transiently co-expressing C4-YFP-HA with B β -Myc, B β ^{S460E}-Myc or B β ^{S460A}-Myc respectively. Total protein extracts were immunoprecipitated with anti-HA antibody, and the anti-Myc antibody was used to detect the indicated proteins in the western blot assay for the indicated proteins. Red numbers indicate the quantitation value from IP product detection in the air or ethylene treatment normalised by their input western blot intensity. (h, i) Ethylene-responsive phenotypes in the roots of representative plants are indicated in the figure. (h) Here, 3-d-old seedlings were grown on Murashige & Skoog (MS) medium containing 2, 5 and 10 μ M aminocyclopropane-1-carboxylic acid (ACC) or without ACC in the dark before being photographed. (i) Measurements of root lengths of the plants indicated in (h). Values are means \pm SD of at least 30 seedlings. Individual data points of root length measurement are plotted. Different letters represent significant differences between each genotype calculated using a two-tailed *t*-test with *P* \leq 0.05.

in vivo co-IP was conducted using 3-d-old etiolated transgenic seedlings treated with or without 4 h of ethylene gas. As shown in Fig. 2(c,d), C4 interacted with both A2 and B β , and the interactions were enhanced by ethylene treatment (Fig. 2c,d). Intriguingly, a previous study found that A2, B β , and C4 were co-

purified by chromatography with a high prominence (Karampelias *et al.*, 2016), which strongly supported our finding that C4 interacts with both A2 and B β to form a PP2A holoenzyme complex.

As the ethylene treatment enhances the B β and C4 interaction and B β undergoes dephosphorylation in response to ethylene, we

aimed to test whether and how the B β phosphorylation status influenced the interaction between B β and C4. In a yeast-two-hybrid assay, we found that the phospho-dead form of B β (B β^{S460A}) strongly interacted with C4, whereas no interaction was detected between C4 and the phospho-mimic form of B β (B β^{S460E}) (Fig. 2e). This result was further supported by a semi *in vivo* co-immunoprecipitation assay of the proteins expressed from tobacco leaves (Fig. 2f). To further validate the interaction *in vivo*, we conducted the co-IP from extracts of protoplasts derived from Col-0 seedlings that were transfected with *C4-YFP-HA/B β -Myc*, *C4-YFP-HA/B β^{S460E} -Myc*, or *C4-YFP-HA/B β^{S460A} -Myc*. Consistent with the *in vitro* assays, the interaction between C4 and B β was enhanced by the dephosphorylation of B β (Fig. 2g), suggesting that the dephosphorylation of B β can potentially enhance the formation of A2-B β -C4 complex.

To further explore whether A2 and C4 subunits function in the ethylene response genetically, we obtained their T-DNA insertion mutants, *a2-1* and *c4-1*, from the *Arabidopsis* Biological Resource Center (Zhou *et al.*, 2004; Spinner *et al.*, 2013) (Fig. S2f,g) and examined their ethylene responses in the presence of various concentrations of ACC. We found that the *c4-1* single mutant displayed a moderate ethylene insensitivity in roots (Fig. 2h,i). Given the fact that C4 interacts with both B β and A2, we then generated *a2-1c4-1* and *b β -1c4-1* double mutants and examined their ethylene responses. The double mutants displayed different degrees of ethylene irresponsiveness in roots (Fig. 2h,i). Notably, the partial ethylene insensitivity observed in *c4-1* roots was significantly enhanced in the *a2-1c4-1* double mutant (Fig. 2h,i). To further confirm the *a2-1c4-1* double mutant phenotype, we generated different alleles of *a2c4* double mutant, named as *a2-1c4-2* and *a2-1c4-3*, using a CRISPR-Cas9 mutagenesis approach to make mutations in *C4* on *a2-1* single mutant background (Fig. S2h). Both alleles displayed a similar root phenotype with that of *a2-1c4-1* in response to ethylene, suggesting that A2 and C4 co-function in the ethylene-mediated root growth inhibition.

A2 and C4 subunits are involved in the ethylene response and EIR1 is the target of A2 subunit

As we screened the potential targets of PP2A by yeast-two-hybrid assay, EIR1 appeared to interact with A2 (Fig. S3a,b). This

interaction was further confirmed by the reciprocal *in vitro* pull-down assays using proteins that were transiently expressed in *Arabidopsis* protoplasts derived from Col-0 plants (Fig. 3a,b). To validate this interaction *in vivo* and to examine whether the interaction was regulated by the ethylene treatment, we generated *A2-FLAG-GFP* transgenic plants and conducted *in vivo* immunoprecipitation in the membrane fractions from root tissues of 3-d-old etiolated seedlings with or without 4 h of ethylene treatment and native antibody against EIR1 was used according to the previous publication (Abas *et al.*, 2006). The interaction between EIR1 and A2 was detected in these plants with or without ethylene treatment, and the interaction between A2 and EIR1 was enhanced in the presence of ethylene (Fig. 3c). Furthermore, different EIR1 species were detected in the samples treated with ethylene compared with that in untreated samples (Fig. 3c). In the absence of ethylene, EIR1 proteins were of higher molecular weight, suggesting that EIR1 is post-translationally modified in response to ethylene.

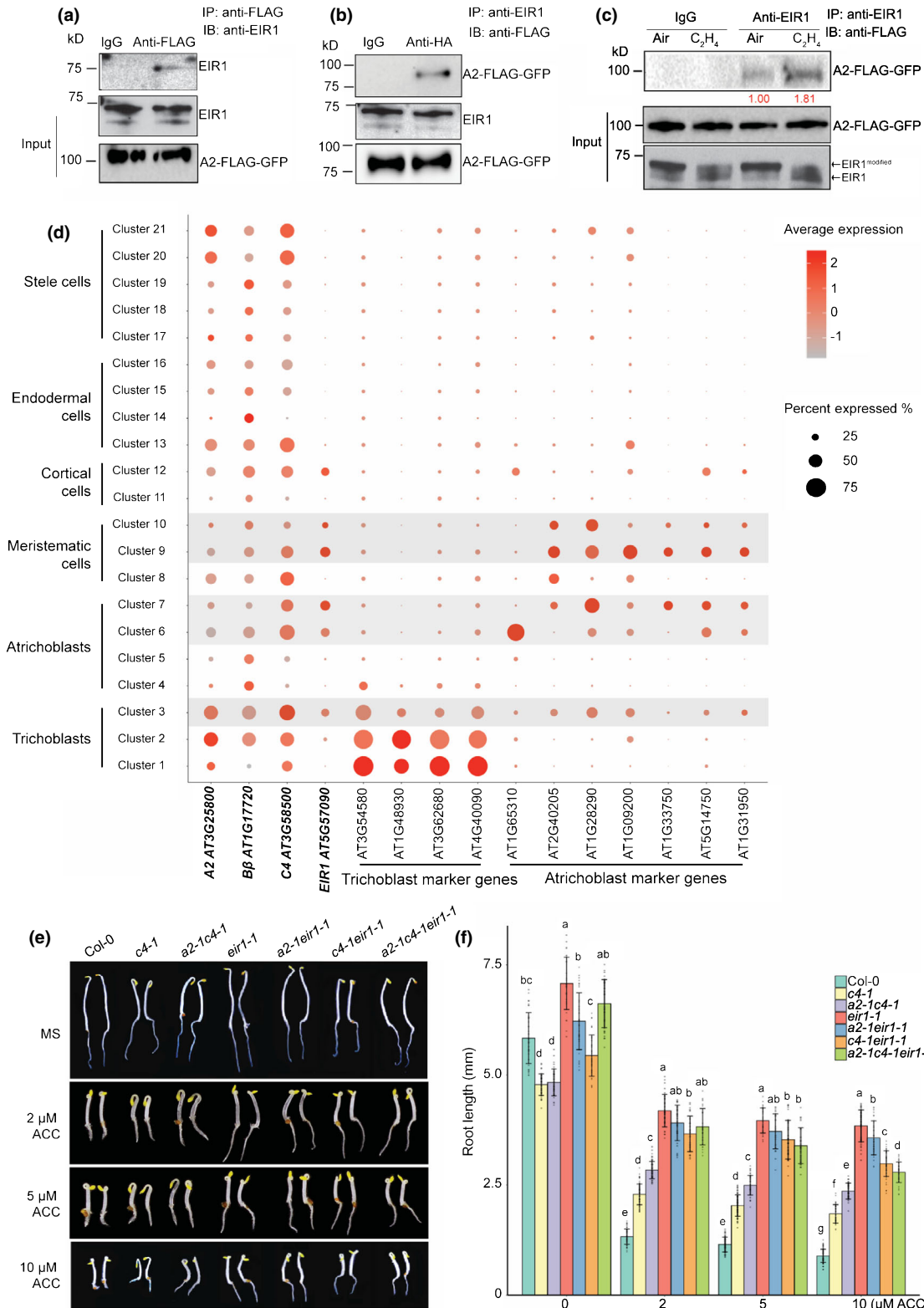
Given the fact that A2 interacts with EIR1 and mutation of *eir1-1* impairs the ethylene response specifically in roots (Roman *et al.*, 1995), we compared the spatial gene expression patterns of *A2*, *C4*, *B β* and *EIR1* in different root cell types using single cell sequencing data that are publicly available (Farmer *et al.*, 2021). We found that *A2*, *C4*, *B β* were expressed across different root cell types (Fig. 3d). When we compared their expression levels and cell-type specificity in different cell clusters, we found that their expression was significantly overlapped with that of *EIR1* in trichoblasts and atrichoblasts (epidermis), and meristematic cells (Figs 3d, S3c,d), providing evidence that A2, C4 and EIR1 could co-function in these root cells. To explore the genetic connections between *EIR1* and *A2* or *C4*, we first compared the phenotypes of *eir1-1* and *a2-1c4-1*. We found that *a2-1c4-1* partially phenocopied *eir1-1* in roots in response to ethylene (Fig. 3e,f). We then generated *a2-1eir1-1*, *c4-1eir1-1* and *a2-1c4-1eir1-1* mutants and examined their ethylene responses in roots. *a2-1eir1-1*, *c4-1eir1-1* and *a2-1c4-1eir1-1* mutants had higher levels of ethylene insensitivity than the respective *a2-1*, *c4-1* and *a2-1c4-1* mutants, with phenotypes that were similar to that of the *eir1-1* mutant (Fig. 3e,f), showing that EIR1 is required for A2 and C4 subunits to regulate the ethylene-mediated root growth inhibition.

Fig. 3 EIR1 is a PP2A target, and A2 and C4 function in ethylene-mediated root growth inhibition via EIR1 in *Arabidopsis*. (a, b) Reciprocal pull-down assays of A2 (A2-FLAG-GFP) with EIR1 transiently expressed in *Arabidopsis* wild-type protoplasts. The total proteins from the protoplasts infected with A2-FLAG-GFP and EIR1 were applied for the pull-down assays using A2 as bait (a) or EIR1 as bait (b). The pull-down products were detected by western blotting using anti-EIR1 antibody (a) or anti-FLAG antibody. (c) *In vivo* co-immunoprecipitation assays of A2 with EIR1. The membrane protein extracts from the roots of 3-d-old etiolated transgenic seedlings carrying 35S::A2-FLAG-GFP treated with 4 h of air or ethylene gas were immunoprecipitated with anti-EIR1. The coimmunoprecipitated A2 proteins were detected by western blotting using anti-FLAG antibody. Red numbers indicate the quantitation value from A2 immunoblot band intensity after immunoprecipitation (IP) normalised to its input western blot intensity under air or ethylene treatment. (d) Spatial expression profiles for A2, B β , C4 and EIR1 in the sNucRNA-seq dataset. Shaded clusters (cluster 3, 6, 7, 9 and 10) indicate the shared cell types expressing four genes. Marker genes that had been previously characterised were used to characterise clusters representing trichoblast and atrichoblast. Dot size represents the percentage of cells in which each gene is expressed (% expressed). Dot colours indicate the average scaled expression of each gene in each cell-type cluster with redder colours representing higher expression levels. (e) Representative Columbia (Col-0), *c4-1*, *a2-1c4-1*, *eir1-1*, *a2-1eir1-1*, *c4-1eir1-1* and *a2-1c4-1eir1-1* mutants were selected for the photograph. Here, 3-d old seedlings were grown on Murashige & Skoog (MS) medium containing 2, 5 and 10 μ M aminocyclopropane-1-carboxylic acid (ACC) or without ACC before being photographed. (f) Measurement of root lengths from the plants indicated in (e). Values are means \pm SD of at least 30 seedlings. Individual root length data are plotted as dots. Different letters indicate significant differences between different genotypes with $P \leq 0.05$ calculated using a two-tailed *t*-test.

A2, C4, and ethylene-induced dephosphorylation of B β are required for EIR1 dephosphorylation

Based on the genetics and biochemistry data, we hypothesised that A2 and C4 regulate EIR1 dephosphorylation in the ethylene

response. To test this idea, we first examined whether the post-translational regulation of EIR1 observed in Fig. 3(c) was protein phosphorylation by treating EIR1 proteins with CIP. After CIP treatment, the higher molecular weight EIR1 in Col-0 without ethylene treatment was barely detectable; whereas, the EIR1 band



patterns in Col-0 treated with ethylene did not show a significant difference from that without CIP treatment (Fig. 4a,b). This result indicated that EIR1 was phosphorylated in the absence of ethylene and that levels of phosphorylation were reduced by ethylene treatment. Next, we compared the EIR1 proteins collected from Col-0 and *a2-1c4-1* root tissues treated with or without ethylene. In Col-0, the EIR1 proteins were phosphorylated without the ethylene treatment; the EIR1 proteins were dephosphorylated with the ethylene treatment. In the *c4-1* and *a2-1c4-1* mutants, however, the phosphorylation of EIR1 was not altered by the ethylene treatment; EIR1 was phosphorylated under both conditions (Fig. 4a). A CIP treatment assay further confirmed that the modification of EIR1 detected in the Col-0 without ethylene treatment and in the *a2-1c4-1* mutant under both conditions was phosphorylation (Fig. 4b). Altogether, these data suggest that, in wild-type plants, EIR1 is phosphorylated in the

absence of ethylene, and its dephosphorylation in the presence of ethylene is dependent on A2 and C4.

Previous studies have shown that the phosphorylation of EIR1 mainly occurs at its central HL region (Michniewicz *et al.*, 2007; Dai *et al.*, 2012; Ganguly *et al.*, 2014). We therefore examined whether the change in EIR1 phosphorylation status in response to ethylene was due to dephosphorylation in this loop. To detect the phosphorylation of EIR1-HL, the purified recombinant GST–EIR1–HL from *in vitro* expression was incubated with the total protein extracted from roots of Col-0 etiolated seedlings treated with air or ethylene and with ^{32}P -ATP. Autoradiography showed that phosphorylated EIR1-HL was detected in the samples from plants with or without ethylene treatment (Fig. 4c); however, the EIR1-HL phosphorylation level was drastically reduced in plants treated with ethylene (Fig. 4c). To further verify that the reduction of EIR1 phosphorylation was regulated by

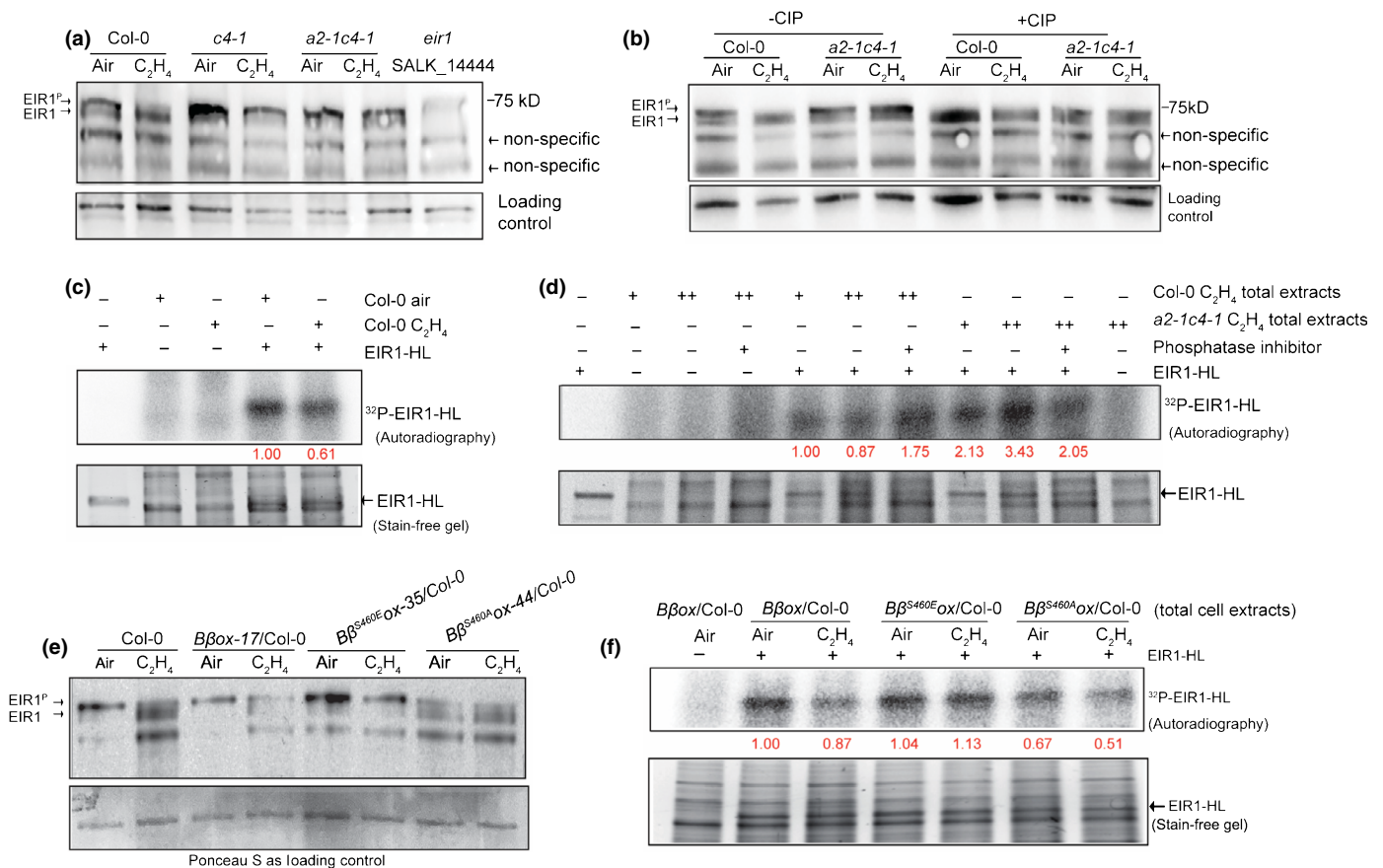


Fig. 4 A2, C4 and $\beta\beta^{S460E}$ are required for EIR1 dephosphorylation in response to ethylene in *Arabidopsis*. (a, b) Western blot for EIR1 phosphorylation status in membrane fractions from the roots of 3-d etiolated Columbia (Col-0) and mutant seedlings treated with calf intestinal alkaline phosphatase (CIP) (b) or not treated with CIP (a) before analysis. Blots were probed with anti-EIR1 antibody. Phosphorylated EIR (EIR1^P) and dephosphorylated EIR are labelled. Nonspecific bands were used to evaluate loading. (c, d) Analysis of *in vitro* phosphorylation of EIR1 from total cell lysates from roots of 3-d etiolated Col-0 seedlings treated with either air or ethylene (c) and seedling of the indicated mutants (d). Red numbers indicate the quantitation value from ^{32}P -EIR1 phosphor intensity divided by the input intensity shown in the stain-free gel. (e) Western blot for EIR1 phosphorylation status in membrane fractions from the roots of 3-d etiolated seedlings indicated in the figure treated with or without ethylene. Blot was probed with anti-EIR1 antibody (upper panel). Ponceau red staining was used as the loading control (bottom panel). (f) *In vitro* autoradiography assay to detect the impact of phosphorylation status of $\beta\beta$ on the phosphorylation of EIR1 in response to ethylene. *In vitro*-purified glutathione-S-transferase (GST)–EIR1–hydrophilic loop (HL) was inoculated with total root cell lysates from 3-d-old etiolated seedlings from the indicated genotypes with or without 4 h of ethylene treatment in the presence of MgCl_2 , ATP and ^{32}P -ATP. The reaction samples were subject to sodium dodecyl sulfate–polyacrylamide gel electrophoresis (SDS-PAGE) and the following autoradiography. Red numbers indicate the quantitation value from autoradiography of ^{32}P -EIR1 phosphor intensity normalised to the input band intensity shown in the stain-free gel. Upper panel: autoradiography; lower panel: stain-free gel as loading control.

A2 and C4 subunits, we examined the phosphorylation of EIR1-HL in total protein extracts from Col-0 seedling and from the *a2-1c4-1* mutant treated with ethylene. The phosphorylation level of EIR1-HL was markedly elevated in the *a2-1c4-1* mutant (Fig. 4d), confirming that ethylene induces the dephosphorylation of EIR1, and that this dephosphorylation is A2 and C4 subunits dependent.

Because ethylene-mediated B β phosphorylation status changing regulates the A2–C4–B β complex formation, and phospho-mimicking B β^{S460E} and phospho-dead B β^{S460A} conferred opposite effects in roots in response to ethylene, we decided to examine whether ethylene-mediated dephosphorylation of B β regulates the EIR1 dephosphorylation in response to ethylene. We introduced *B $\beta^{S460A}ox$* and *B $\beta^{S460E}ox$* into the *eir1-1* mutant to generate *B $\beta^{S460A}ox/eir1-1$* and *B $\beta^{S460E}ox/eir1-1$* , and examined their ethylene response in roots. We found that the phenotypes conferred by *B $\beta^{S460A}ox$* and *B $\beta^{S460E}ox$* were completely impaired in *B $\beta^{S460A}ox/eir1-1$* and *B $\beta^{S460E}ox/eir1-1$* , and the plants displayed the *eir1-1* phenotype (Fig. S4a,b), showing that EIR1 is required for B β to regulate root growth in response to ethylene. We then conducted an immunoblot assay to examine whether B β phosphorylation status regulated the phosphorylation of EIR1 protein. In *B βox* plants, the changes in EIR1 phosphorylation in response to ethylene were similar to that in Col-0 (Fig. 4e). In the *B $\beta^{S460E}ox$* plants, the majority of EIR1 proteins was phosphorylated in the absence of ethylene, but phosphorylation was not altered by ethylene treatment (Fig. 4e). By contrast, the EIR1 proteins were largely dephosphorylated in the *B $\beta^{S460A}ox$* plants even without ethylene treatment, and the phosphorylation level was similar to that in the wild-type plants or in the *B βox* plants that had been treated with ethylene (Fig. 4e). We then conducted an *in vitro* EIR1-HL phosphorylation assay by inoculating the *in vitro*-purified EIR1-HL with the total protein extracts from the plants of *B βox* , *B $\beta^{S460A}ox$* or *B $\beta^{S460E}ox$* treated with or without ethylene. We found that the phosphorylation level of EIR-HL was decreased by the ethylene treatment or by *B $\beta^{S460A}ox$* (Fig. 4f). The ethylene-induced reduction of EIR-HL phosphorylation level was impaired in *B $\beta^{S460E}ox$* . All together, these data demonstrated that the ethylene-induced dephosphorylation of B β led to dephosphorylation of EIR1.

B β regulates PP2A-mediated EIR1 dephosphorylation in a manner that depends on A2 and C4 subunits

The A subunit of PP2A is a scaffolding protein that mediates the formation of PP2A holoenzyme (Shi, 2009). We speculated that A2 and C4 are required for the regulation of B β on the dephosphorylation of EIR1 in response to ethylene. To test this possibility, we first introduced B β^{S460A} or B β^{S460E} into the *a2-1c4-1bb-1* triple mutant to generate *B $\beta^{S460A}ox/a2-1c4-1bb-1$* and *B $\beta^{S460E}ox/a2-1c4-1bb-1$* plants; we then compared their root growth with the roots of *a2-1c4-1*, *B $\beta^{S460E}ox/Col-0$* , and *B $\beta^{S460A}ox/Col-0$* in response to ethylene. We found that the roots of *B $\beta^{S460A}ox/a2-1c4-1bb-1$* and of *B $\beta^{S460E}ox/a2-1c4-1bb-1$* had

phenotypes similar to the roots of *a2-1c4-1bb-1* mutant (Fig. 5a). The enhanced ethylene-induced root growth inhibition in *B $\beta^{S460A}ox/Col-0$* and the ethylene insensitivity in root growth in *B $\beta^{S460E}ox/Col-0$* were impaired in the absence of A2 and C4 (Fig. 5a), providing genetic evidence that A2 and C4 are required for the function of B β in response to ethylene. Furthermore, EIR1 dephosphorylation induced by ethylene treatment or by the *B $\beta^{S460A}ox$* was eliminated in the absence of A2 and C4 (Fig. 5b,c), supporting the conclusion that A2 and C4 are required for B β to regulate PP2A activity on EIR1 dephosphorylation in response to ethylene.

Based on the data presented above, a model is emerging that A2 mediates the PP2A assembly on the target EIR1 and that the phosphorylation status of B β regulates the assembly and the activity of PP2A complex composed of A2, C4, and B β , which in turn dephosphorylates EIR1. To test this hypothesis, we conducted co-IP assays to examine whether EIR1 was part of the A2–C4–B β complex and whether the phosphorylation status of B β would alter the assembly of the complex on EIR1. We first generated the *a2-1bb-1c4-1eir1-1* quadruple mutant to eradicate the interruptive effects of endogenous A2, B β , C4 and EIR1 proteins. We then introduced various combinations of subunits and B β mutants into the protoplasts derived from the *a2-1bb-1c4-1eir1-1* plants: *A2-FLAG-GFP*, *C4-YFP-HA*, *EIR1* and *B β -Myc*; *A2-FLAG-GFP*, *C4-YFP-HA*, *EIR1* and *B β^{S460A} -Myc*; or *A2-FLAG-GFP*, *C4-YFP-HA*, *EIR1* and *B β^{S460E} -Myc*. The infected protoplasts were then treated with or without 4 h of 10 μ M ACC before testing. All the proteins were well expressed in the *in vitro* assembly system (Fig. 5d). Importantly, the ethylene-induced dephosphorylation of EIR1 in the assay was similar to that detected in the Col-0 plants when the four wild-type proteins were expressed (Fig. 5d), showing that the exogenous proteins functioned properly in the *in vitro* assembly system. We also noticed that the majority of EIR1 was dephosphorylated when the phospho-dead B β^{S460A} was expressed, whereas the majority of EIR1 was phosphorylated when the phospho-mimic B β^{S460E} was expressed (Fig. 5d). Using A2 as bait, the co-IP assay showed that B β , C4, and EIR1 were in the same protein complex (Fig. 5d). In the absence of ACC treatment or when B β was constitutively phosphorylated (B β^{S460E}), the interaction of the protein complex is weakened (Fig. 5d). By contrast, the complex formation was enhanced in the presence of ACC or when B β was constitutively dephosphorylated (B β^{S460A}) (Fig. 5d). We then examined how A2 regulates the A2–B β –C4–EIR1 protein complex interaction and the phosphorylation of EIR1 by co-IP in the absence of A2. Under these conditions and using C4 as bait, the interaction between B β and C4 was still detectable; however, no EIR1 was detected in the immunoprecipitated products. Furthermore, in the absence of A2, very little dephosphorylated EIR1 was detected from the protoplasts that expressed wild-type B β with ACC treatment or in protoplasts that expressed phospho-dead *B β^{S460A}* (Fig. 5e). These results demonstrated that A2 as a scaffolding protein is required for the assembly and the phosphatase activity of PP2A on EIR1.

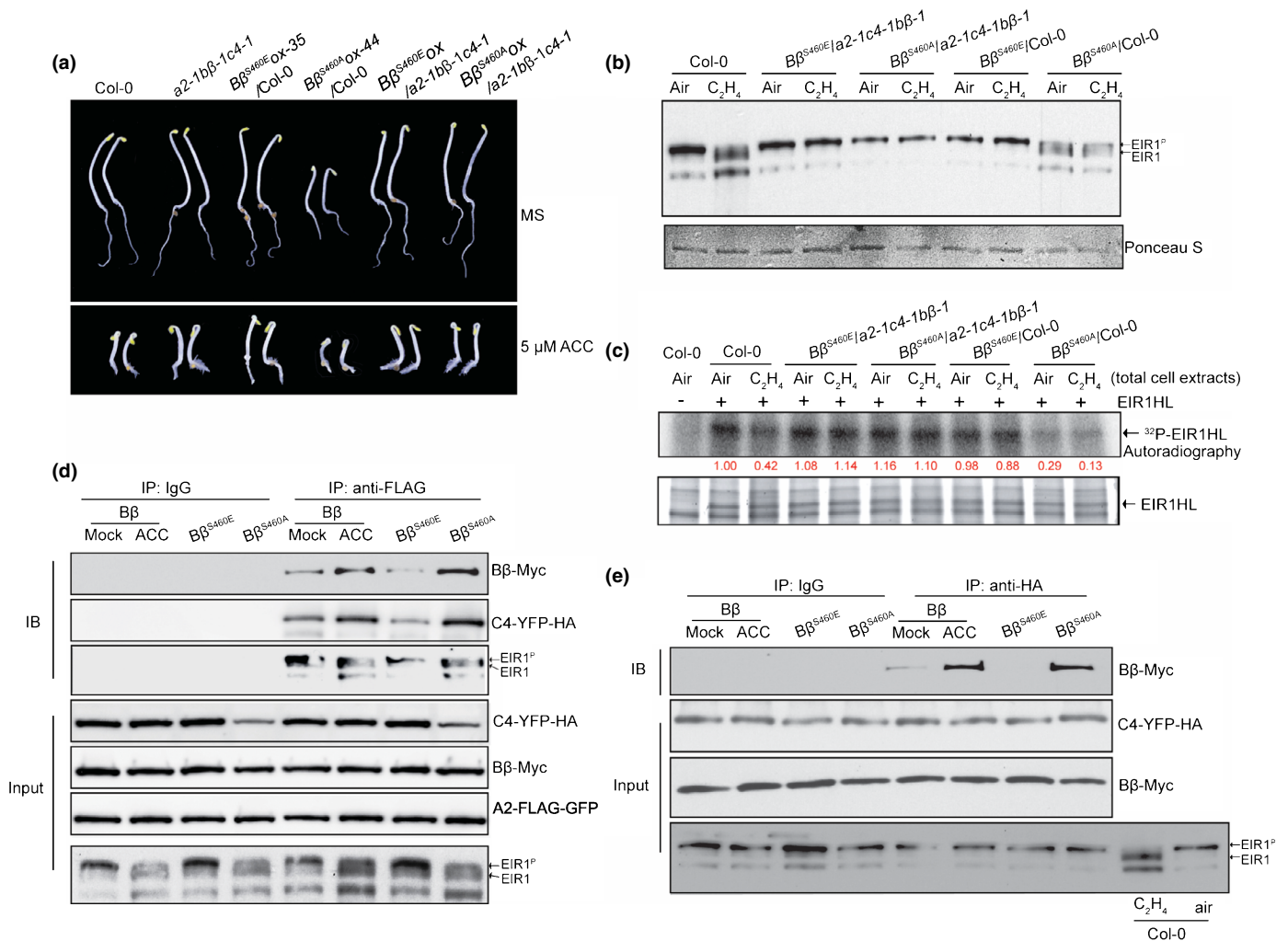


Fig. 5 Ethylene-dependent dephosphorylation of EIR1 requires A2, C4 and dephosphorylated Bβ in *Arabidopsis*. (a) The seedling phenotype of the plants indicated in the figure. Here, 3-d-old etiolated transgenic seedlings were grown on Murashige & Skoog (MS) medium containing 5 μM aminocyclopropane-1-carboxylic acid (ACC) or without ACC in the dark before photographed. (b) Western blot analysis of EIR1 phosphorylation status in membrane fractions of Columbia (*Col-0*), *Bβ^{S460E}ox/a2-1bβ-1c4-1*, *Bβ^{S460A}ox/a2-1bβ-1c4-1*, *Bβ^{S460E}ox/Col-0*, and *Bβ^{S460A}ox/Col-0* 3-d-old seedlings treated with or without ethylene. EIR1 was detected with anti-EIR1 antibody (upper panel). Ponceau red staining is used as the loading control (bottom panel). (c) *In vitro* autoradiography assay to examine the function of A2 and C4 in Bβ-regulated EIR1 phosphorylation. *In vitro*-purified glutathione-S-transferase (GST)-EIR1-hydrophilic loop (HL) was inoculated with total root cell lysates from 3-d-old etiolated seedlings of indicated genotypes in the presence of purified GST-EIR1-HL, MgCl₂, ATP and ³²P-ATP. The reaction samples were subject to sodium dodecyl sulfate-polyacrylamide gel electrophoresis (SDS-PAGE) and the following autoradiography. Red numbers indicate the quantitation value of individual ³²P-EIR1 phosphor band intensity normalised to the corresponding input band intensity in each lane shown in the stain-free gel. Upper panel: autoradiography. Lower panel: stain-free gel as loading control. (d) Western blot analysis of the total cell extracts from the *a2-1bβ-1c4-1eir1-1* protoplasts that transiently co-expressed A2-FLAG-GFP, C4-YFP-HA, and EIR1 as well as Bβ-Myc, Bβ^{S460E}-Myc, or Bβ^{S460A}-Myc immunoprecipitated with anti-FLAG antibody. (e) Western blot analysis of total cell extracts from the *a2-1bβ-1c4-1eir1-1* protoplasts that transiently co-expressed C4-YFP-HA, and EIR1 as well as Bβ-Myc, Bβ^{S460E}-Myc, or Bβ^{S460A}-Myc immunoprecipitated with anti-HA antibody.

Dephosphorylation of Bβ leads to an activation of EIR1-mediated auxin transport in epidermis in response to ethylene

One way of how EIR1 exclusively restricts root growth is through EIR1-mediated auxin distribution. Loss of function of EIR1 is ethylene insensitive in roots. But our biochemistry and cellular biology data revealed that the EIR1 dephosphorylation in ethylene treatment and EIR1 polarity was not altered by ethylene treatment (Fig. S5). As dephosphorylation of Bβ led to

dephosphorylation of EIR1, resulting in root growth inhibition, we speculated that the EIR1-mediated auxin distribution will be regulated by the phosphorylation status of Bβ. To test this idea, we introduced *DR5::GFP*, the proxy of auxin distribution, into *eir1-1*, *a2-1c4-1*, *Bβ^{S460E}ox* and *Bβ^{S460A}ox*, we then examined the *DR5::GFP* expression in the plants with or without ethylene treatment and in plants growing on MS medium and MS medium supplied with 1 μM ACC. We found that the expression of *DR5::GFP* was limited to the root tip and root cap in the PP2A *a2-1c4-1* double mutant under ethylene treatment or on the

ACC-containing medium (Fig. 6a,b), and ethylene-induced ectopic expression of *DR5::GFP* in epidermis in Col-0 was impaired in the *a2-1c4-1* mutant (Fig. 6a,b), which was similar to that in the *eir1-1* mutant (Fig. 6a,b). However, in the $B\beta^{S460A}$ *ox* plants, in which EIR1 is constitutively dephosphorylated, *DR5::GFP* expression was clearly induced in epidermis even in the absence of ethylene or ACC. By contrast, *DR5::GFP* expression was restricted to the root tips and root cap in the $B\beta^{S460E}$ *ox* plants, in which EIR1 was constitutively phosphorylated, and ethylene-induced ectopic expression of *DR5::GFP*, proxy of auxin distribution, in the epidermis was impaired in the $B\beta^{S460E}$ *ox* plants. Fluorescence intensity measurements in epidermal cells in the elongation zone in different genetic backgrounds confirmed our observation that ethylene-mediated auxin transport in the elongation zone was disrupted in *eir1-1*, *a2-1c4-1*, and $B\beta^{S460E}$ *ox* (Fig. 6c–e). Because auxin distribution is important for the plant gravitropic response, we then carried out a gravity response assay. We found that *a2-1c4-1* and $B\beta^{S460E}$ *ox* roots, in which the EIR1 fails to undergo a phosphorylation change, had a gravitropic defect. The angles of root gravitropic bending for wild-type plants were *c.* 90° after 24 h gravistimulation, and for *eir1-1* were *c.* 50°. Similar to *eir1-1*, *a2-1c4-1*, and $B\beta^{S460E}$ *ox* exhibited obvious decreases in bending with the angles ranging from 60° to 70° (Fig. S6). These data, together with the result for *DR5::GFP* expression, demonstrated that dephosphorylated EIR1 is critical to proper auxin transport in the epidermis in the elongation zone in response to ethylene, which requires activation of the PP2A A2–C4–B β complex by B β dephosphorylation.

Putting all these results together, our data supported a model that, in the absence of ethylene, phosphorylated B β at Ser460 destabilises and subsequently deactivates the PP2A complex of A2, C4, and B β , resulting in EIR1 phosphorylation, preventing auxin transport in epidermis, and resulting in normal root growth (Fig. 7). In the presence of ethylene, dephosphorylated B β stabilises the A2–C4–B β complex, switching on the PP2A activity to dephosphorylate EIR1, activating auxin transport in the epidermis, and resulting in ethylene-mediated root growth inhibition (Fig. 7).

Discussion

The PP2A holoenzyme consists of the PP2A core enzyme and a regulatory subunit. The A and C subunits form the PP2A core enzyme, and the regulatory B subunit is the main modulator for PP2A holoenzyme and elicits temporal and spatial specificity. The *Arabidopsis* genome sequence predicts the existence of up to 255 heterotrimeric PP2A isoforms; genes encoding five C subunits, three A subunits, and 17 B subunits have been annotated (Zhou *et al.*, 2004). Although the PP2A core enzyme is relatively invariable, the various and interchangeable regulatory B subunits result in a diversity of distinct PP2A holoenzymes. PP2A has been shown to be involved in numerous biological processes (Skottke *et al.*, 2011; Tang *et al.*, 2011; Segonzac *et al.*, 2014; Waadt *et al.*, 2015; Karampelias *et al.*, 2016; Wang *et al.*, 2016; Yue *et al.*, 2016; Booker & DeLong, 2017; Bu *et al.*, 2017; Zhao *et al.*, 2019; Bian *et al.*, 2020; Tan *et al.*, 2020). However, the

mechanisms governing the assembly of a distinct PP2A complex to regulate a specific target in a particular biological event are still largely unknown. In this study, we have provided multiple lines of compelling evidence that ethylene-mediated dephosphorylation of B β switches on the PP2A A2–C4–B β activity, which dephosphorylates EIR1, promoting auxin transport in the epidermis, leading to ethylene-induced root growth inhibition (Fig. 7). First, our data from biochemistry and genetic experiments revealed that B β is dephosphorylated at Ser460 by ethylene treatment, and that B β constitutive phosphorylation repressed, whereas B β constitutive dephosphorylation enhanced, ethylene-mediated root growth inhibition (Fig. 1). Second, we showed that the PP2A subunit C4 interacts with PP2A A2 and B β subunits both *in vitro* and *in vivo*, and that dephosphorylation of B β regulates the formation of the A2–C4–B β complex (Fig. 2). Third, we demonstrated that EIR1 is one of the targets of PP2A, and that A2 mediates the interaction between A2 and EIR1 (Fig. 3). Our genetics data provide a strong piece of evidence that A2, C4 and B β function in the same protein complex with EIR1. Biochemistry data showed that ethylene-induced dephosphorylation of B β led to the activation of PP2A to dephosphorylate EIR1 (Figs 4, 5). Finally, we demonstrated that, in the absence of ethylene, phosphorylation of B β destabilised the complex of A2, B β , and C4 and EIR1 remained phosphorylated, preventing auxin transport in the epidermis, and leading to normal root growth (Figs 5, 6). The dephosphorylation of B β in the presence of ethylene switches on PP2A activity, resulting in dephosphorylation of EIR1, promoting auxin transport in the epidermis to inhibit root growth (Figs 5, 6).

The B subunit was believed to determine substrate specificity (Janssens *et al.*, 2008; Shi, 2009; Uhrig *et al.*, 2013). However, no direct interaction between B β and the substrate EIR1 was detected (Fig. S3b). Instead, we discovered that the scaffolding subunit A2 directly interacts with EIR1, even in the absence of ethylene (Fig. 3). The dephosphorylation of the regulatory subunit B β modulates its interaction with the catalytic subunit C4, leading to an enhanced interaction of these three subunits to assemble the PP2A holoenzyme, and therefore activating PP2A function on the dephosphorylation of EIR1 in the presence of ethylene. In this case, it is possible that, in the absence of ethylene, phosphorylated B β blocks its interaction with C4 to maintain a low level of PP2A activity, therefore preventing the dephosphorylation of EIR1. The interaction between A2 and C4 potentially provides a ready state for PP2A activation. Upon the ethylene treatment, dephosphorylated B β can immediately tighten the interaction of the core enzyme A2–C4 and activate its function to dephosphorylate EIR1, which provides an efficient regulation on the specific target in response to the plant hormone ethylene.

It has been proposed that, through auxin modulation, ethylene is capable of specifically inhibiting the growth of expanding cells or reducing cell proliferation (Swarup *et al.*, 2007; Street *et al.*, 2015). Vaseva *et al.* (2018) found that the epidermis is the main site of ethylene action controlling plant growth in both roots and shoots. However, the molecular mechanisms are still not clear. Our findings fill one of the gaps between ethylene-mediated root

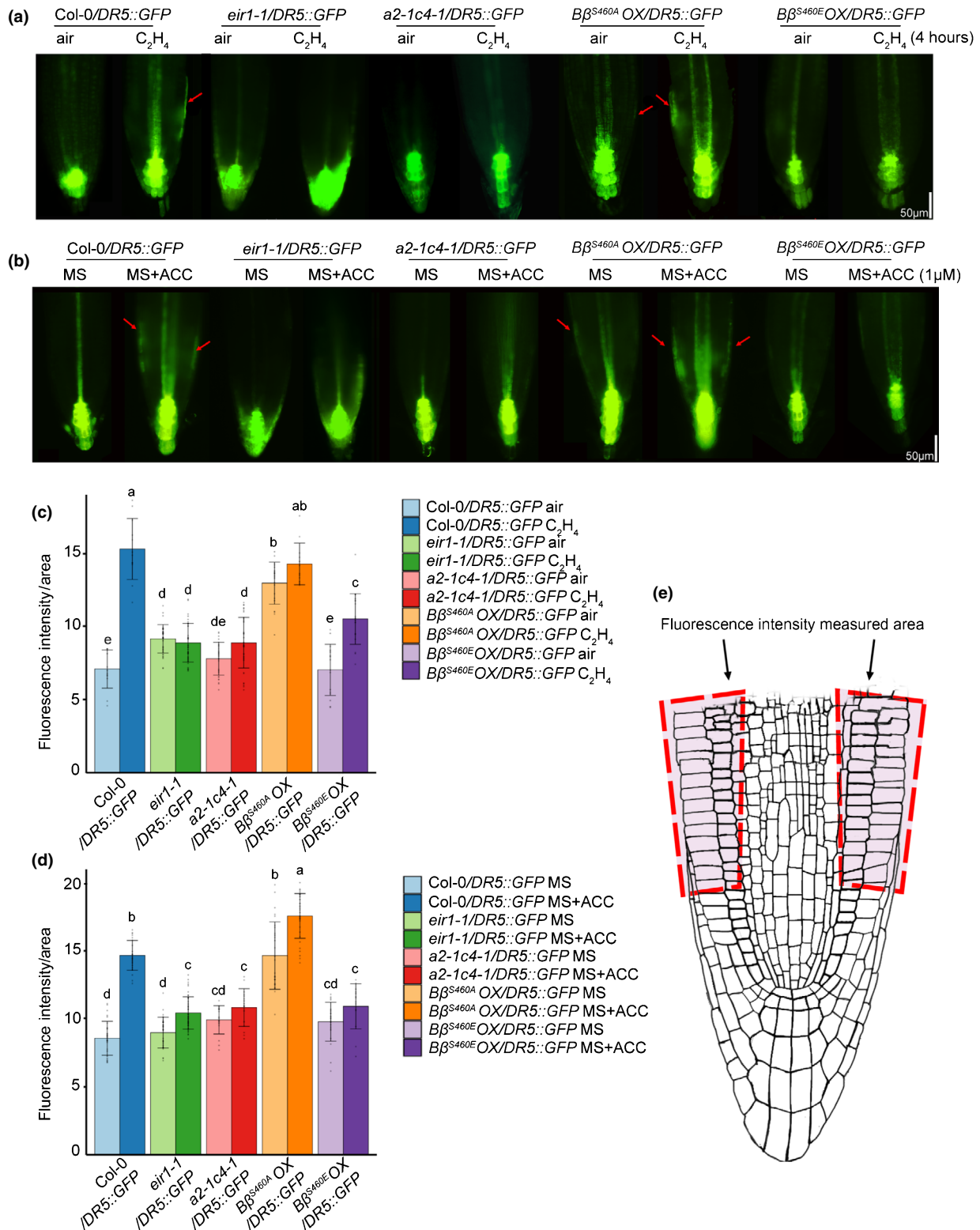


Fig. 6 Mutations in PP2A inhibit auxin transport in epidermis in elongation zone in response to ethylene in *Arabidopsis*. (a, b) *DR5::GFP* expression in the roots of the plants indicated in the figure with ethylene or aminocyclopropane-1-carboxylic acid (ACC) treatment. Representative root fluorescence microscope images are displayed. Seedlings were grown on Murashige & Skoog (MS) medium for 3 d in the dark and photographed after 4 h of 10 ppm ethylene gas or control air treatment (a). Seedlings were grown on medium with or without 1 μM ACC in the dark for 3 d before being photographed (b). Red arrows indicate the epidermal cells with induced *DR5::GFP* fluorescence signals. Bars, 50 μm . (c, d) Measurement of fluorescence intensity per area in the epidermis in the indicated plants under each indicated treatment conditions. Individual measurement data are plotted as dots. Different letters indicate significant differences between different genotypes and treatments with $P \leq 0.05$ calculated by a two-tailed *t*-test. Values are means \pm SD of at least 20 seedlings. (e) Root model to indicate root epidermal cells in the elongation zone used for fluorescence measurement.

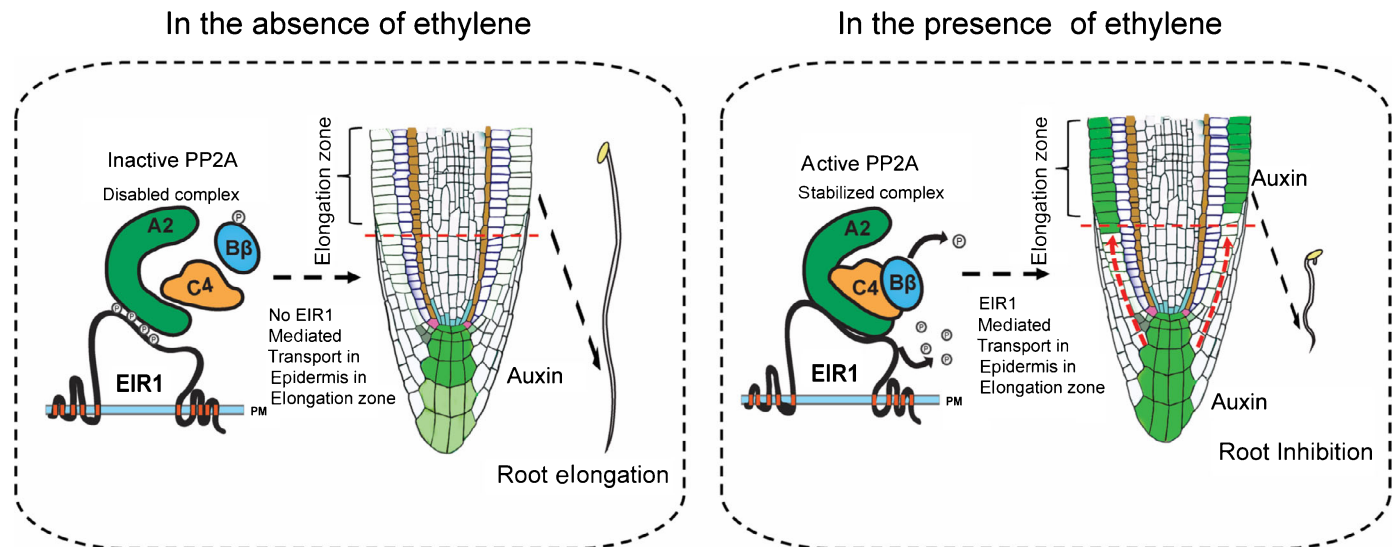


Fig. 7 A model to illustrate how ethylene regulates B β dephosphorylation to switch on PP2A to dephosphorylate EIR1, leading to root growth inhibition in *Arabidopsis*. Left panel: In the absence of ethylene, phosphorylated B β destabilises and deactivates the PP2A complex composed of A2, B β and C4. Phosphorylated EIR1 due to PP2A inactivation prevents auxin transport into the epidermis in the root elongation zone, promoting root elongation. Right panel: In the presence of ethylene, dephosphorylated B β stabilises the A2–C4–B β complex, switching on the PP2A activity to dephosphorylate EIR1, activating auxin transport in the epidermis, and resulting in ethylene-mediated root growth inhibition.

growth inhibition and EIR1-mediated auxin transport in the epidermis in the elongation zone. In the presence of ethylene, B β is phosphorylated, switching on PP2A to dephosphorylate EIR1, promoting auxin transport in the epidermis in the elongation zone, as a result root growth is inhibited. EIR1 was identified as ETHYLENE INSENSITIVE ROOT 1 (also as known as PIN2), whose ethylene insensitivity is restricted in roots (Alonso *et al.*, 2003). The phosphorylation of EIR1 is regulated by different plant hormones and nutrient factors (Rahman *et al.*, 2010; Wang *et al.*, 2019; Yuan *et al.*, 2020; Otvos *et al.*, 2021). Otvos *et al.* (2021) found that nitrate induced PIN2 dephosphorylation, which affected auxin flux via polarised localisation at the plasma membrane. A very recent study showed that salicylic acid inhibits PP2A activity, leading to PIN2 hyperphosphorylation, resulting in an increased internalisation and a reduced polar membrane localisation of PIN2 (Tan *et al.*, 2020). Particularly, the PP2A A1 subunit is responsible for the dephosphorylation of PIN2 in the absence of SA and PIN2 phosphorylation after SA treatment occurs at its HL region, which is important for the intracellular trafficking of PIN2 (Ganguly *et al.*, 2014). Unlike salicylic acid, ethylene enhances the activity of PP2A, specifically with the composition of A2–C4–B β , to dephosphorylate EIR1. More interestingly, this ethylene-regulated phosphorylation also occurs at the HL region (Fig. 4). However, the ethylene-induced phosphorylation change in EIR1 did not alter the polarity of EIR1 (Fig. S5), which is consistent with a previous publication (Méndez-Bravo *et al.*, 2019), suggesting that ethylene and SA or nitrogen potentially act at different phosphorylation sites of EIR1 to achieve their specific regulations. For ethylene treatment, it is possible that dephosphorylation at specific residues of EIR1 prohibited its biochemical function rather than its polar membrane localisation to inhibit auxin transport in the epidermis. Identifying the ethylene-regulated phosphorylation sites of EIR1 by

phosphoproteomic analysis and further analysis of the biochemical impacts of ethylene-induced dephosphorylation on EIR1 will be the future interests.

Acknowledgements

We thank C. Luschnig for sharing native anti-EIR1 antibody and C. Jo and A. Basnet for plant and laboratory maintenance. We thank D. Kelley for sharing *DR5::GFP* seeds. We thank J. Xu for sharing *EIR1-GFP* transgenic plants. We thank the Arabidopsis Biological Resource Center for providing seeds. ZS was supported by the Graduate Continuing Fellowship from The University of Texas at Austin. This work was supported by grants from the National Institute of Health to HQ (NIH-2R01 GM115879-01).

Competing interests

None declared.

Author contributions

Conceptualisation, ZS, BZ and HQ; Methodology, ZS, BZ, XC, KB and HQ; Investigation, ZS, BZ, PK, JGB, JT, MK and KB; Writing – Original Draft, HQ; Writing – Review and Editing, ZS, KB and HQ; Visualisation, ZS and HQ; Supervision, HQ; Funding Acquisition, HQ.

ORCID

Karen S. Browning [ID https://orcid.org/0000-0003-0348-7996](https://orcid.org/0000-0003-0348-7996)
 Jackson G. Burns [ID https://orcid.org/0000-0001-9558-1239](https://orcid.org/0000-0001-9558-1239)
 Xu Chen [ID https://orcid.org/0000-0002-5166-083X](https://orcid.org/0000-0002-5166-083X)

Meiyu Ke  <https://orcid.org/0000-0001-9472-1674>
 Prashanth Kotla  <https://orcid.org/0000-0001-8104-5822>
 Hong Qiao  <https://orcid.org/0000-0003-3359-1962>
 Zhengyao Shao  <https://orcid.org/0000-0003-2965-8335>
 Jaclyn Tran  <https://orcid.org/0000-0002-9094-6080>
 Bo Zhao  <https://orcid.org/0000-0002-3016-4749>

Data availability

Further information and requests for reagents and all unique materials generated in this study may be directed to and will be fulfilled by the corresponding author Hong Qiao (hqiao@austin.utexas.edu).

References

- Abas L, Benjamins R, Malenica N, Paciorek T, Wiśniewska J, Moulinier-Anzola JC, Sieberer T, Friml J, Luschnig C. 2006. Intracellular trafficking and proteolysis of the *Arabidopsis* auxin-efflux facilitator PIN2 are involved in root gravitropism. *Nature Cell Biology* 8: 249–256.
- Abas L, Luschnig C. 2010. Maximum yields of microsomal-type membranes from small amounts of plant material without requiring ultracentrifugation. *Analytical Biochemistry* 401: 217–227.
- Achard P, Baghour M, Chapple A, Hedden P, Van Der Straeten D, Genschik P, Moritz T, Harberd NP. 2007. The plant stress hormone ethylene controls floral transition via DELLA-dependent regulation of floral meristem-identity genes. *Proceedings of the National Academy of Sciences, USA* 104: 6484–6489.
- Alonso JM, Hirayama T, Roman G, Nourizadeh S, Ecker JR. 1999. EIN2, a bifunctional transducer of ethylene and stress responses in *Arabidopsis*. *Science* 284: 2148–2152.
- Alonso JM, Stepanova AN, Solano R, Wisman E, Ferrari S, Ausubel FM, Ecker JR. 2003. Five components of the ethylene-response pathway identified in a screen for weak ethylene-insensitive mutants in *Arabidopsis*. *Proceedings of the National Academy of Sciences, USA* 100: 2992–2997.
- Avila JR, Lee JS, Torii KU. 2015. Co-immunoprecipitation of membrane-bound receptors. *The Arabidopsis Book* 2015: e0180.
- Bian C, Guo X, Zhang Y, Wang L, Xu T, DeLong A, Dong J. 2020. Protein phosphatase 2A promotes stomatal development by stabilizing SPEECHLESS in *Arabidopsis*. *Proceedings of the National Academy of Sciences, USA* 117: 13127–13137.
- Bleecker AB, Kende H. 2000. Ethylene: a gaseous signal molecule in plants. *Annual Review of Cell and Developmental Biology* 16: 1–18.
- Booker MA, DeLong A. 2017. Atypical protein phosphatase 2A gene families do not expand via paleopolyploidization. *Plant Physiology* 173: 1283–1300.
- Boutrot F, Segonzac C, Chang KN, Qiao H, Ecker JR, Zipfel C, Rathjen JP. 2010. Direct transcriptional control of the *Arabidopsis* immune receptor FLS2 by the ethylene-dependent transcription factors EIN3 and EIL1. *Proceedings of the National Academy of Sciences, USA* 107: 14502–14507.
- Broekgaarden C, Caarls L, Vos IA, Pieterse CM, Van Wees SC. 2015. Ethylene: traffic controller on hormonal crossroads to defense. *Plant Physiology* 169: 2371–2379.
- Brumos J, Robles LM, Yun J, Vu TC, Jackson S, Alonso JM, Stepanova AN. 2018. Local auxin biosynthesis is a key regulator of plant development. *Developmental Cell* 47: 306–318.
- Bu SL, Liu C, Liu N, Zhao JL, Ai LF, Chi H, Li KL, Chien CW, Burlingame AL, Zhang SW *et al.* 2017. Immunopurification and mass spectrometry identifies protein phosphatase 2A (PP2A) and BIN2/GSK3 as regulators of AKS transcription factors in *Arabidopsis*. *Molecular Plant* 10: 345–348.
- Butler A, Hoffman P, Smibert P, Papalexis E, Satija R. 2018. Integrating single-cell transcriptomic data across different conditions, technologies, and species. *Nature Biotechnology* 36: 411–420.
- Chang C, Bleecker AB. 2004. Ethylene biology. More than a gas. *Plant Physiology* 136: 2895–2899.
- Chang C, Kwok SF, Bleecker AB, Meyerowitz EM. 1993. *Arabidopsis* ethylene-response gene ETR1: similarity of product to two-component regulators. *Science* 262: 539–544.
- Chang J, Li X, Fu W, Wang J, Yong Y, Shi H, Ding Z, Kui H, Gou X, He K *et al.* 2019. Asymmetric distribution of cytokinins determines root hydrotropism in *Arabidopsis thaliana*. *Cell Research* 29: 984–993.
- Chang KN, Zhong S, Weirauch MT, Hon G, Pelizzola M, Li H, Huang S-SC, Schmitz RJ, Urlich MA, Kuo D *et al.* 2013. Temporal transcriptional response to ethylene gas drives growth hormone cross-regulation in *Arabidopsis*. *eLife* 2: e00675.
- Chao Q, Rothenberg M, Solano R, Roman G, Terzaghi W, Ecker JR. 1997. Activation of the ethylene gas response pathway in *Arabidopsis* by the nuclear protein ETHYLENE-INSENSITIVE3 and related proteins. *Cell* 89: 1133–1144.
- Clark KL, Larsen PB, Wang X, Chang C. 1998. Association of the *Arabidopsis* CTR1 Raf-like kinase with the ETR1 and ERS ethylene receptors. *Proceedings of the National Academy of Sciences, USA* 95: 5401–5406.
- Dai M, Zhang C, Kania U, Chen F, Xue Q, McCray T, Li G, Qin G, Wakeley M, Terzaghi W *et al.* 2012. A PP6-type phosphatase holoenzyme directly regulates PIN phosphorylation and auxin efflux in *Arabidopsis*. *Plant Cell* 24: 2497–2514.
- DeLong A. 2006. Switching the flip: protein phosphatase roles in signaling pathways. *Current Opinion in Plant Biology* 9: 470–477.
- Dubois M, Van den Broeck L, Claeys H, Van Vlierberghe K, Matsui M, Inzé D. 2015. The ETHYLENE RESPONSE FACTORS ERF6 and ERF11 antagonistically regulate mannitol-induced growth inhibition in *Arabidopsis*. *Plant Physiology* 169: 166–179.
- Ecker JR. 1995. The ethylene signal transduction pathway in plants. *Science* 268: 667–675.
- Farmer A, Thibivilliers S, Ryu KH, Schiefelbein J, Libault M. 2021. Single-nucleus RNA and ATAC sequencing reveals the impact of chromatin accessibility on gene expression in *Arabidopsis* roots at the single-cell level. *Molecular Plant* 14: 372–383.
- Fukao T, Xu K, Ronald PC, Bailey-Serres J. 2006. A variable cluster of ethylene response factor-like genes regulates metabolic and developmental acclimation responses to submergence in rice. *Plant Cell* 18: 2021–2034.
- Ganguly A, Park M, Kesawat MS, Cho H-T. 2014. Functional analysis of the hydrophilic loop in intracellular trafficking of *Arabidopsis* PIN-FORMED proteins. *Plant Cell* 26: 1570–1585.
- Gao Z, Chen YF, Randlett MD, Zhao XC, Findell JL, Kieber JJ, Schaller GE. 2003. Localization of the Raf-like kinase CTR1 to the endoplasmic reticulum of *Arabidopsis* through participation in ethylene receptor signaling complexes. *The Journal of Biological Chemistry* 278: 34725–34732.
- Gong Y, Allassimone J, Varnau R, Sharma N, Cheung LS, Bergmann DC. 2021. Tuning self-renewal in the *Arabidopsis* stomatal lineage by hormone and nutrient regulation of asymmetric cell division. *eLife* 10: e63335.
- Guo H, Ecker JR. 2003. Plant responses to ethylene gas are mediated by SCF^{EBF1/EBF2}-dependent proteolysis of EIN3 transcription factor. *Cell* 115: 667–677.
- Han L, Li G-J, Yang K-Y, Mao G, Wang R, Liu Y, Zhang S. 2010. Mitogen-activated protein kinase 3 and 6 regulate Botrytis cinerea-induced ethylene production in *Arabidopsis*. *The Plant Journal* 64: 114–127.
- Hartman S, Liu Z, van Veen H, Vicente J, Reinen E, Martopawiro S, Zhang H, van Dongen N, Bosman F, Bassel GW *et al.* 2019. Ethylene-mediated nitric oxide depletion pre-adapts plants to hypoxia stress. *Nature Communications* 10: 4020.
- Haydon MJ, Mielczarek O, Frank A, Román Á, Webb AAR. 2017. Sucrose and ethylene signaling interact to modulate the circadian clock. *Plant Physiology* 175: 947–958.
- Hua J, Meyerowitz EM. 1998. Ethylene responses are negatively regulated by a receptor gene family in *Arabidopsis thaliana*. *Cell* 94: 261–271.
- Hua J, Sakai H, Nourizadeh S, Chen QG, Bleecker AB, Ecker JR, Meyerowitz EM. 1998. EIN4 and ERS2 are members of the putative ethylene receptor gene family in *Arabidopsis*. *Plant Cell* 10: 1321–1332.
- Jackson MB. 2008. Ethylene-promoted elongation: an adaptation to submergence stress. *Annals of Botany* 101: 229–248.

- Janssens V, Longin S, Goris J. 2008. PP2A holoenzyme assembly: in cauda venenum (the sting is in the tail). *Trends in Biochemical Sciences* 33: 113–121.
- Joo S, Liu Y, Lueth A, Zhang S. 2008. MAPK phosphorylation-induced stabilization of ACS6 protein is mediated by the non-catalytic C-terminal domain, which also contains the *cis*-determinant for rapid degradation by the 26S proteasome pathway. *The Plant Journal* 54: 129–140.
- Ju C, Yoon GM, Shemansky JM, Lin DY, Ying ZI, Chang J, Garrett WM, Kessenbrock M, Groth G, Tucker ML *et al.* 2012. CTR1 phosphorylates the central regulator EIN2 to control ethylene hormone signaling from the ER membrane to the nucleus in *Arabidopsis*. *Proceedings of the National Academy of Sciences, USA* 109: 19486–19491.
- Karampelias M, Neyt P, De Groeve S, Aesaert S, Coussens G, Rolčík J, Bruno L, De Winne N, Van Minnebruggen A, Van Montagu M *et al.* 2016. ROTUNDA3 function in plant development by phosphatase 2A-mediated regulation of auxin transporter recycling. *Proceedings of the National Academy of Sciences, USA* 113: 2768–2773.
- Kieber JJ, Rothenberg M, Roman G, Feldmann KA, Ecker JR. 1993. CTR1, a negative regulator of the ethylene response pathway in *Arabidopsis*, encodes a member of the raf family of protein kinases. *Cell* 72: 427–441.
- Leitner J, Luschnig C. 2014. Ubiquitylation-mediated control of polar auxin transport: analysis of *Arabidopsis* PIN2 auxin transport protein. In: Otegui MS, ed. *Plant endosomes: methods and protocols*. New York, NY, USA: Springer New York, 233–249.
- Li G, Meng X, Wang R, Mao G, Han L, Liu Y, Zhang S. 2012. Dual-level regulation of ACC synthase activity by MPK3/MPK6 cascade and its downstream WRKY transcription factor during ethylene induction in *Arabidopsis*. *PLoS Genetics* 8: e1002767.
- Licausi F, van Dongen JT, Giuntoli B, Novi G, Santaniello A, Geigenberger P, Perata P. 2010. HRE1 and HRE2, two hypoxia-inducible ethylene response factors, affect anaerobic responses in *Arabidopsis thaliana*. *The Plant Journal* 62: 302–315.
- Luschnig C, Gaxiola RA, Grisafi P, Fink GR. 1998. EIR1, a root-specific protein involved in auxin transport, is required for gravitropism in *Arabidopsis thaliana*. *Genes & Development* 12: 2175–2187.
- Ma B, He S-J, Duan K-X, Yin C-C, Chen H, Yang C, Xiong Q, Song Q-X, Lu X, Chen H-W *et al.* 2013. Identification of rice ethylene-response mutants and characterization of MHZ7/OsEIN2 in distinct ethylene response and yield trait regulation. *Molecular Plant* 6: 1830–1848.
- Marhavý P, Kurenda A, Siddique S, Dénervaud Tendon V, Zhou F, Holbein J, Hasan MS, Grundler FM, Farmer EE, Geldner N. 2019. Single-cell damage elicits regional, nematode-restricting ethylene responses in roots. *EMBO Journal* 38: e100972.
- Méndez-Bravo A, Ruiz-Herrera LF, Cruz-Ramírez A, Guzman P, Martínez-Trujillo M, Ortiz-Castro R, López-Bucio J. 2019. CONSTITUTIVE TRIPLE RESPONSE1 and PIN2 act in a coordinate manner to support the indeterminate root growth and meristem cell proliferating activity in *Arabidopsis* seedlings. *Plant Science* 280: 175–186.
- Mersmann S, Bourdais G, Rietz S, Robatzek S. 2010. Ethylene signaling regulates accumulation of the FLS2 receptor and is required for the oxidative burst contributing to plant immunity. *Plant Physiology* 154: 391–400.
- Michniewicz M, Zago MK, Abas L, Weijers D, Schweighofer A, Meskiene I, Heisler MG, Ohno C, Zhang J, Huang F *et al.* 2007. Antagonistic regulation of PIN phosphorylation by PP2A and PINOID directs auxin flux. *Cell* 130: 1044–1056.
- Minkenberg B, Zhang J, Xie K, Yang Y. 2019. CRISPR-PLANT v.2: an online resource for highly specific guide RNA spacers based on improved off-target analysis. *Plant Biotechnology Journal* 17: 5–8.
- Neff MM, Neff JD, Chory J, Pepper AE. 1998. dCAPS, a simple technique for the genetic analysis of single nucleotide polymorphisms: experimental applications in *Arabidopsis thaliana* genetics. *The Plant Journal* 14: 387–392.
- Otvos K, Marconi M, Vega A, O'Brien J, Johnson A, Abualia R, Antonielli L, Montesinos JC, Zhang Y, Tan S *et al.* 2021. Modulation of plant root growth by nitrogen source-defined regulation of polar auxin transport. *EMBO Journal* 40: e106862.
- Pandey BK, Huang G, Bhosale R, Hartman S, Sturrock CJ, Jose L, Martin OC, Karady M, Voosenek LACJ, Ljung K *et al.* 2021. Plant roots sense soil compaction through restricted ethylene diffusion. *Science* 371: 276–280.
- Qiao H, Shen Z, S-c H, Schmitz RJ, Ulrich MA, Briggs SP, Ecker JR. 2012. Processing and subcellular trafficking of ER-tethered EIN2 control response to ethylene gas. *Science* 338: 390–393.
- Qing D, Yang Z, Li M, Wong WS, Guo G, Liu S, Guo H, Li N. 2016. Quantitative and functional phosphoproteomic analysis reveals that ethylene regulates water transport via the C-terminal phosphorylation of aquaporin PIP2;1 in *Arabidopsis*. *Molecular Plant* 9: 158–174.
- Rahman A, Takahashi M, Shibasaki K, Wu S, Inaba T, Tsurumi S, Baskin TI. 2010. Gravitropism of *Arabidopsis thaliana* roots requires the polarization of PIN2 toward the root tip in meristematic cortical cells. *Plant Cell* 22: 1762–1776.
- Rodgers JT, Vogel RO, Puigserver P. 2011. Clk2 and B56 β mediate insulin-regulated assembly of the PP2A phosphatase holoenzyme complex on Akt. *Molecular Cell* 41: 471–479.
- Roman G, Lubarsky B, Kieber JJ, Rothenberg M, Ecker JR. 1995. Genetic analysis of ethylene signal transduction in *Arabidopsis thaliana*: five novel mutant loci integrated into a stress response pathway. *Genetics* 139: 1393–1409.
- Růžicka K, Ljung K, Vanneste S, Podhorská R, Beeckman T, Friml J, Benková E. 2007. Ethylene regulates root growth through effects on auxin biosynthesis and transport-dependent auxin distribution. *Plant Cell* 19: 2197–2212.
- Schindelin J, Arganda-Carreras I, Frise E, Kaynig V, Longair M, Pietzsch T, Preibisch S, Rueden C, Saalfeld S, Schmid B *et al.* 2012. Fiji: an open-source platform for biological-image analysis. *Nature Methods* 9: 676–682.
- Segonzac C, Macho AP, Sanmartín M, Ntoukakis V, Sánchez-Serrano JJ, Zipfel C. 2014. Negative control of BAK1 by protein phosphatase 2A during plant innate immunity. *EMBO Journal* 33: 2069–2079.
- Shi H, Liu R, Xue C, Shen X, Wei N, Deng XW, Zhong S. 2016. Seedlings transduce the depth and mechanical pressure of covering soil using COP1 and ethylene to regulate EBF1/EBF2 for soil emergence. *Current Biology* 26: 139–149.
- Shi Y. 2009. Serine/threonine phosphatases: mechanism through structure. *Cell* 139: 468–484.
- Skottke KR, Yoon GM, Kieber JJ, DeLong A. 2011. Protein phosphatase 2A controls ethylene biosynthesis by differentially regulating the turnover of ACC synthase isoforms. *PLoS Genetics* 7: e1001370.
- Spinner L, Gadeyne A, Belcram K, Goussot M, Moison M, Duroc Y, Eeckhout D, De Winne N, Schaefer E, Van De Slijke E *et al.* 2013. A protein phosphatase 2A complex spatially controls plant cell division. *Nature Communications* 4: 1863.
- Steffens B, Kovalev A, Gorb SN, Sauter M. 2012. Emerging roots alter epidermal cell fate through mechanical and reactive oxygen species signaling. *Plant Cell* 24: 3296–3306.
- Street IH, Aman S, Zubo Y, Ramzan A, Wang X, Shakeel SN, Kieber JJ, Schaller GE. 2015. Ethylene inhibits cell proliferation of the *Arabidopsis* root meristem. *Plant Physiology* 169: 338–350.
- Swarup R, Perry P, Hagenbeek D, Van Der Straeten D, Beecher GT, Sandberg G, Bhalerao R, Ljung K, Bennett MJ. 2007. Ethylene upregulates auxin biosynthesis in *Arabidopsis* seedlings to enhance inhibition of root cell elongation. *Plant Cell* 19: 2186–2196.
- Tan S, Abas M, Verstraeten I, Glanc M, Molnár G, Hajný J, Lasák P, Petřík I, Russinova E, Petrášek J *et al.* 2020. Salicylic acid targets protein phosphatase 2A to attenuate growth in plants. *Current Biology* 30: 381–395.
- Tang W, Yuan M, Wang R, Yang Y, Wang C, Osés-Prieto JA, Kim T-W, Zhou H-W, Deng Z, Gampala SS *et al.* 2011. PP2A activates brassinosteroid-responsive gene expression and plant growth by dephosphorylating BZR1. *Nature Cell Biology* 13: 124–131.
- Uhrig RG, Labandera A-M, Moorhead GB. 2013. *Arabidopsis* PPP family of serine/threonine protein phosphatases: many targets but few engines. *Trends in Plant Science* 18: 505–513.
- Vaseva II, Qudeimat E, Potuschak T, Du Y, Genschik P, Vandenbussche F, Van Der Straeten D. 2018. The plant hormone ethylene restricts *Arabidopsis* growth via the epidermis. *Proceedings of the National Academy of Sciences, USA* 115: E4130–E4139.
- Waadt R, Manalansan B, Rauniyar N, Munemasa S, Booker MA, Brandt B, Waadt C, Nusinow DA, Kay SA, Kunz H-H *et al.* 2015. Identification of open stomatal-1-interacting proteins reveals interactions with sucrose non-

- fermenting1-related protein kinases2 and with Type 2A protein phosphatases that function in abscisic acid responses. *Plant Physiology* 169: 760–779.
- Wang L, Ko EE, Tran J, Qiao H. 2020a. TREE1-EIN3-mediated transcriptional repression inhibits shoot growth in response to ethylene. *Proceedings of the National Academy of Sciences, USA* 117: 29178–29189.
- Wang L, Zhang F, Rode S, Chin KK, Ko EE, Kim J, Iyer VR, Qiao H. 2017. Ethylene induces combinatorial effects of histone H3 acetylation in gene expression in *Arabidopsis*. *BMC Genomics* 18: 538.
- Wang L, Zhang Z, Zhang F, Shao Z, Zhao B, Huang A, Tran J, Hernandez FV, Qiao H. 2020b. EIN2-directed histone acetylation requires EIN3-mediated positive feedback regulation in response to ethylene. *Plant Cell* 33: 322–337.
- Wang P, Shen L, Guo J, Jing W, Qu Y, Li W, Bi R, Xuan W, Zhang Q, Zhang W. 2019. Phosphatidic acid directly regulates PINOID-dependent phosphorylation and activation of the PIN-FORMED2 auxin efflux transporter in response to salt stress. *Plant Cell* 31: 250–271.
- Wang R, Liu M, Yuan M, Oses-Prieto JA, Cai X, Sun Y, Burlingame AL, Wang ZY, Tang W. 2016. The brassinosteroid-activated BRI1 receptor kinase is switched off by dephosphorylation mediated by cytoplasm-localized PP2A B' subunits. *Molecular Plant* 9: 148–157.
- Wang ZP, Xing HL, Dong L, Zhang HY, Han CY, Wang XC, Chen QJ. 2015. Egg cell-specific promoter-controlled CRISPR/Cas9 efficiently generates homozygous mutants for multiple target genes in *Arabidopsis* in a single generation. *Genome Biology* 16: 144.
- Wu Q, Kuang K, Lyu M, Zhao Y, Li Y, Li J, Pan Y, Shi H, Zhong S. 2020. Allosteric deactivation of PIFs and EIN3 by microproteins in light control of plant development. *Proceedings of the National Academy of Sciences, USA* 117: 18858–18868.
- Xu K, Xu X, Fukao T, Canlas P, Maghirang-Rodriguez R, Heuer S, Ismail AM, Bailey-Serres J, Ronald PC, Mackill DJ. 2006. Sub1A is an ethylene-response-factor-like gene that confers submergence tolerance to rice. *Nature* 442: 705–708.
- Yoo S-D, Cho Y-H, Sheen J. 2007. *Arabidopsis* mesophyll protoplasts: a versatile cell system for transient gene expression analysis. *Nature Protocols* 2: 1565–1572.
- Yuan X, Xu P, Yu Y, Xiong Y. 2020. Glucose-TOR signaling regulates PIN2 stability to orchestrate auxin gradient and cell expansion in *Arabidopsis* root. *Proceedings of the National Academy of Sciences, USA* 117: 32223–32225.
- Yue K, Sandal P, Williams EL, Murphy E, Stes E, Nikonorova N, Ramakrishna P, Czyzewicz N, Montero-Morales L, Kumpf R *et al.* 2016. PP2A-3 interacts with ACR4 and regulates formative cell division in the *Arabidopsis* root. *Proceedings of the National Academy of Sciences, USA* 113: 1447–1452.
- Zhang F, Qi B, Wang L, Zhao B, Rode S, Riggan ND, Ecker JR, Qiao H. 2016a. EIN2-dependent regulation of acetylation of histone H3K14 and non-canonical histone H3K23 in ethylene signalling. *Nature Communications* 7: 13018.
- Zhang F, Wang L, Lim JY, Kim T, Pyo Y, Sung S, Shin C, Qiao H. 2016b. Phosphorylation of CBP20 links microRNA to root growth in the ethylene response. *PLoS Genetics* 12: e1006437.
- Zhang F, Wang L, Qi B, Zhao B, Ko EE, Riggan ND, Chin K, Qiao H. 2017. EIN2 mediates direct regulation of histone acetylation in the ethylene response. *Proceedings of the National Academy of Sciences, USA* 114: 10274–10279.
- Zhao J-L, Zhang L-Q, Liu N, Xu S-L, Yue Z-L, Zhang L-L, Deng Z-P, Burlingame AL, Sun D-Y, Wang Z-Y *et al.* 2019. Mutual regulation of receptor-like kinase SIT1 and B'k-PP2A shapes the early response of rice to salt stress. *Plant Cell* 31: 2131–2151.
- Zhou H-W, Nussbaumer C, Chao Y, DeLong A. 2004. Disparate roles for the regulatory A subunit isoforms in *Arabidopsis* protein phosphatase 2A. *Plant Cell* 16: 709–722.

Supporting Information

Additional Supporting Information may be found online in the Supporting Information section at the end of the article.

Fig. S1 B β expression pattern, PP2A B β T-DNA insertion mutant, and protein expression levels of B β ox/Col-0, B β ^{S460E}ox/Col-0 or B β ^{S460A}ox/Col-0 in *Arabidopsis*.

Fig. S2 The interactions between B β and C4 or C4 and A2, expression patterns of A2, B β , and C4 and PP2A a2 and c4 mutants in *Arabidopsis*.

Fig. S3 EIR1 interacts with A2 and the UMAP visualisations of spatial expression profiles for A2, B β , C4 and EIR1 in sNucRNA-seq in *Arabidopsis*.

Fig. S4 B β regulates root inhibition through EIR1 in response to ethylene in *Arabidopsis*.

Fig. S5 The subcellular localisation of EIR1 with or without ethylene treatment in *Arabidopsis*.

Fig. S6 The gravitropism assays of Col-0, *eir1-1*, *a2-1c4-1*, and B β ^{S460E}ox/Col-0 in *Arabidopsis*.

Table S1 List of primers.

Please note: Wiley Blackwell are not responsible for the content or functionality of any Supporting Information supplied by the authors. Any queries (other than missing material) should be directed to the *New Phytologist* Central Office.